AME599 Combustion Chemistry and Physics

Lecture 3

3. Basic Chemical Kinetics

In Lecture 1, we learned that thermodynamics determines the "ideal" end state of a reaction process. It does not tell us, however, how fast the reaction proceeds and whether under a particular reaction condition, the reaction can proceed to the equilibrium state. Answers to these questions are left to chemical kinetics. This is the topic of the current lecture.

3.1. Chemical Reaction Rate

3.1.1 Global Versus Elementary Reactions

So far all reactions we have discussed are called global reactions. These reactions described an overall process by which reactants are converted to anticipated products at the end of the process. They do not describe the actual physical process. Take, for example, the simple reaction of hydrogen oxidation:

$$2\,H_2 + O_2 \rightarrow 2\,H_2O\ .$$

Physically this reaction is almost impossible since it would require two H_2 molecules and one O_2 molecules to simultaneously collide, and while they collide the three molecules have align themselves in a way that two water molecules may be produced. Statistically this is a very unlikely event.

The above discussion leads us to define a class of reactions known as elementary reactions. These are the reactions that take place physically, e.g., the combination of two $H\bullet$ atoms to form H_2

$$H\bullet + H\bullet \rightarrow H_2.$$

Obviously the formation of the H_2 molecule requires the two $H\bullet$ atoms to physically "touch" each other. In the gas phase this is done by atom-atom *collision*. The dissociation of the H_2 molecule

$$H_2 \rightarrow H\bullet + H\bullet$$

is also an elementary reaction. Since the above two reactions describe a reversible reaction process, we often write the reaction as

$$H\bullet + H\bullet \leftrightarrows H_2\ .$$

Unlike global reactions, all elementary reactions are *reversible*.

3.1.2 Elementary Reaction Type and Reaction Rates

As we discussed above, elementary reactions have two key characteristics. First, the reactant molecules will have to physically collide with each other for the reaction to take place. Second the reaction must be reversible. There are only a few types of reactions that satisfy these criteria.

The first type of elementary reactions is known as the *unimolecular* reaction, which involves only one reactant:

$$A \rightarrow \text{products.} \tag{3.1}$$

Examples include bond breaking reactions and isomerization reactions. As we will learn later, a unimolecular reaction actually requires collision so the first criterion is not violated. The rate of the above reaction is proportional to the molar concentration of A, i.e.,

$$-\frac{d[A]}{dt} = k[A] \ . \tag{3.2}$$

Here the bracket [] denotes molar concentration (mol/cm^3) and the proportionality k (1/s) is the *reaction rate constant*. If A is the only species in the reactor and k is a constant during the reaction process, the concentration of A can be easily determined,

$$[A]_t = [A]_0 e^{-kt} \ . \tag{3.3}$$

where $[A]_0$ is the initial concentration ($t = 0$).

For reasons to be discussed later, the rate constant of most unimolecular reactions is dependent on the total molar concentration of the species in a reactor. We shall denote the total concentration as $[M]$. At low pressures, we often observe that k is directly proportional to $[M]$.[†] For this reason, we sometimes write a unimolecular reaction as

$$A + M \rightarrow \text{products} + M \tag{3.4}$$

where M denotes all other gas molecules in the reactor. The reaction rate is expressed by

$$-\frac{d[A]}{dt} = k^{'}[A][M] \ , \tag{3.5}$$

where $k^{'} = k/[M]$.

[†] Note that under the ideal gas condition the total molar concentration $[\mathrm{M}] = p/R_uT$. Therefore the proportionality of k to $[M]$ is equivalent to its proportionality to pressure at a given temperature.

Reactions of type (3.2) are known as the first-order reaction, and reactions in the form of (3.4) are known as the second-order reactions.

The second type of elementary reactions is called bimolecular reactions. They are generally expressed by

$$A + B \rightarrow \text{products.} \tag{3.6}$$

The reaction rate is given by

$$-\frac{d[A]}{dt} = -\frac{d[B]}{dt} = k[A][B] \ . \tag{3.7}$$

Again, the proportionality k (cm^3/mol-s) is the rate constant. In general, analytical solutions do not exist for the dependence of [A] or [B] on reaction time, except for the following two special cases. In case I, we have $A = B$, so the reaction is

$$A + A \text{ (or } 2A) \rightarrow \text{products.} \tag{3.8}$$

The reaction rate is

$$-\frac{1}{2}\frac{d[A]}{dt} = k[A]^2 \ . \tag{3.9}$$

Again, this type of reactions is sometime called the second order reactions, since the reaction rate is the second order in reactant concentration. Assuming that k is a constant during the reaction process, we integrate Eq. (3.9) to yield

$$[A]_t = \frac{[A]_0}{1 + 2kt[A]_0} \ . \tag{3.10}$$

In case II, we have $[B]_0 \gg [A]_0$ so the concentration of [B] is only infinitesimally perturbed even if A is completely consumed. We may therefore assume $k' \cong k[B]_0$ = constant and obtain

$$[A]_t = [A]_0 e^{-k't} = [A]_0 e^{-k[B]_0 t} \ . \tag{3.11}$$

This type of reaction is sometimes called the pseudo-first order reaction.

Termolecular reactions are rare, as they require the simultaneous collision and encounter of three molecules,

$$A + B + C \rightarrow \text{products}. \tag{3.12}$$

The reaction rate is given by

$$-\frac{d[A]}{dt} = -\frac{d[B]}{dt} = -\frac{d[C]}{dt} = k[A][B][C] \ . \tag{3.13}$$

where k has the units of cm^6/mol-s.

3.1.3 The Law of Mass Action

Since all elementary reactions are reversible, we may write the forward and back rates for an arbitrary reaction

$$A + B \leftrightarrows \mathrm{C} + \mathrm{D}$$

as

$$R_{forward} = R_f = k_f[A][B] \ , \tag{3.14f}$$

$$R_{back} = R_b = k_b[C][D] \ . \tag{3.14b}$$

The net reaction rate is

$$-\frac{d[A]}{dt} = -\frac{d[B]}{dt} = \frac{d[C]}{dt} = \frac{d[D]}{dt} = R_f - R_b = k_f[A][B] - k_b[C][D] \ . \tag{3.15}$$

When the reaction reaches chemical equilibrium, the net rate goes to zero, but as we discussed earlier, the forward and back reactions proceed at finite and equal rates, i.e.,

$$R_f - R_b = k_f[A]_{eq}[B]_{eq} - k_b[C]_{eq}[D]_{eq} = 0 \ .$$

It follows that

$$\frac{k_f}{k_b} = \frac{[C]_{eq}[D]_{eq}}{[A]_{eq}[B]_{eq}} \ . \tag{3.16}$$

Since the right-hand side of Eq. (3.16) is the equilibrium constant K_c itself, we have

$$K_c = \frac{k_f}{k_b} \ . \tag{3.17}$$

Equation (3.17) states that the forward and back reaction rate constants are related to the equilibrium constant, and they do not have to be independently determined if the thermochemical data of A, B, C, and D or the equilibrium constant is known. In general, k_b is calculated from k_f via the equilibrium constant, and vice versa. In addition, Eq. (3.17) is applicable to reaction conditions with or without equilibrium, since the equation does not contain species concentration.

3.1.4 Chain Reactions and Steady State Assumption

In the following classical example, we shall demonstrate the importance of a collection of elementary reactions in forming a chain reaction sequence that carry the overall reaction to completion. We shall also illustrate an important assumption used in chemical kinetics analysis, known as the steady-state assumption.

It was observed that at low reaction conversions the rate of HBr production from the reaction of H_2 and Br_2 follows a $[\mathrm{Br}]^{1/2}$ dependence. Obviously, a direct reaction given by

$$H_2 + Br_2 \rightarrow 2HBr \qquad (3.18)$$

cannot explain the square root dependence of the reaction rate on the Br concentration. To explain the odd relationship between the reaction rates and reactant concentration, a *chain reaction mechanism* had to be postulated,

$$Br_2 \rightarrow 2Br\bullet \qquad \text{(chain initiation)} \qquad (3.19f)$$
$$Br\bullet + H_2 \rightarrow HBr + H\bullet \qquad \text{(chain propagation)} \qquad (3.20f)$$
$$H\bullet + HBr \rightarrow H_2 + Br\bullet \qquad \text{(chain propagation)} \qquad (3.20b)$$
$$H\bullet + Br_2 \rightarrow HBr + Br\bullet \qquad \text{(chain propagation)} \qquad (3.21)$$
$$Br\bullet + Br\bullet \rightarrow Br_2 \qquad \text{(chain termination)} \qquad (3.19b)$$

The reverse of reaction (3.21), and the combinations of 2 H• atoms and of H• and Br• are negligibly slow and thus are excluded in the postulated mechanism. The above reaction sequence may also be depicted as shown in Figure 3.1.

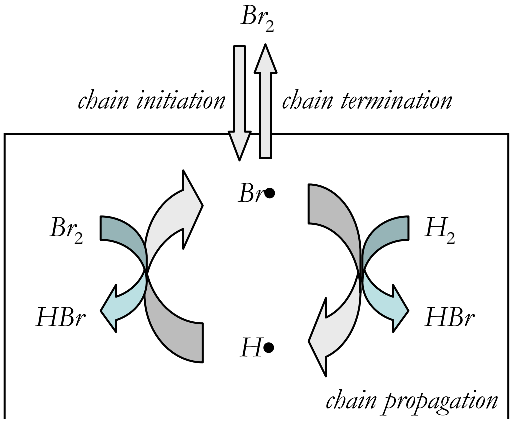

Figure 3.1 Free radical chain reactions in H_2 and Br_2 reactions.

The chain reaction sequence starts with step (3.19f), which produces the $Br\bullet$ atoms. This step is called the *chain initiation* step. The Br• atom is a free radical species and is extremely reactive. It can readily attack one of the reactants, i.e., molecular hydrogen (H_2), to yield HBr and an $H\bullet$ atom (step 3.20f). This reaction step is reversible, in that the back reaction (3.20b) can proceed at a rapid rate to compete with the forward reaction step (3.20f). The $H\bullet$ atom would attack the second reactants (*Br*$_2$) to yield *HBr* and re-generate the *Br*• atom (step 3.21), which attacks more *H*$_2$. In this way, a chain reaction cycle is established with the free-radical species *H*• and *Br*• being the *chain carriers*. The reaction steps (3.20f), (3.20b), and (3.21) are called the *chain propagation* reactions, since there is no net production or destruction of the chain carriers.

The destruction of the reactants *H*$_2$ and *Br*$_2$ and the production of *HBr* is completely facilitate by the aforementioned chain cycle unless one or more free radical carriers is destroyed by a *chain termination* step. Chain termination can be due to radical-radical recombination, radical-molecule reaction to yield a less-reactive radical, or radical quenching by a reactor wall. Here the chain termination is caused by the recombination of 2 *Br*• atoms to regenerate Br$_2$, which is the reverse of the chain initiation itself.

We may write the production rates of the chain carriers as

$$\frac{d[Br\bullet]}{dt}=2k_{19f}[Br_2]-k_{20f}[Br\bullet][H_2]+k_{20b}[HBr][H\bullet]+k_{21}[H\bullet][Br_2]-2k_{19b}[Br\bullet]^2 \quad .(3.20)$$

$$\frac{d[H\bullet]}{dt}=k_{20f}[Br\bullet][H_2]-k_{20b}[HBr][H\bullet]-k_{21}[H\bullet][Br_2] \quad . \qquad (3.21)$$

Since both H• and Br• are extremely reactive, they cannot accumulate in the reactor. In other words, as soon as a Br• atom is produced, it will react immediately with H$_2$ or recombine into Br$_2$. As such the net rate of production of these free-radical species is close to zero. This assumption is known as the *steady-state* assumption.

Under the steady state assumption, we may re-write Eqs. (3.20) and (3.21) as

$$2k_{19f}[Br_2]-k_{20f}[Br\bullet]_{ss}[H_2]+k_{20b}[HBr][H\bullet]_{ss}+k_{21}[H\bullet]_{ss}[Br_2]-2k_{19b}[Br\bullet]_{ss}^2=0 \quad ,(3.22)$$

$$k_{20f}[Br\bullet]_{ss}[H_2]-k_{20b}[HBr][H\bullet]_{ss}-k_{21}[H\bullet]_{ss}[Br_2]=0 \quad , \qquad (3.23)$$

where the subscript "*ss*" denotes the steady state. We may solve for $[H\bullet]_{ss}$ and $[Br\bullet]_{ss}$ to yield

$$[Br\bullet]_{ss}=\sqrt{\frac{k_{19f}}{k_{19b}}[Br_2]} \quad , \qquad (3.24)$$

$$[H\bullet]_{ss}=\sqrt{\frac{k_{19f}}{k_{19b}}[Br_2]}\,\frac{k_{20f}[H_2]}{k_{20b}[HBr]+k_{21}[Br_2]} \quad . \qquad (3.25)$$

Then the rate of *HBr* production is

$$\begin{aligned}\frac{d[HBr]}{dt} &\cong k_{20f}[Br\bullet]_{ss}[H_2]-k_{20b}[HBr][H\bullet]_{ss}+k_{21}[H\bullet]_{ss}[Br_2] \\ &= 2k_{20f}\sqrt{\frac{k_{19f}}{k_{19b}}}[H_2]\sqrt{[Br_2]}\left(1+\frac{k_{20b}[HBr]}{k_{21}[Br_2]}\right)^{-1}\end{aligned} \quad . \tag{3.26a}$$

Of course, at low reaction conversion (i.e., $[HBr] \sim 0$), we have

$$\frac{d[HBr]}{dt} \cong= 2k_{20f}\sqrt{\frac{k_{19f}}{k_{19b}}}[H_2]\sqrt{[Br_2]} \ , \tag{3.26b}$$

which explains the experimental observation for the $[Br_2]^{1/2}$ dependence.

Here we learned two important concepts. The first is the chain reaction and its importance in explaining a seemingly simple reaction system. The second is the steady state assumption, where the net production rates of free radicals or other relatively reactive species may be assumed to be zero in the analysis of chain reactions.

Although the reaction between H_2 and Br_2 is dictated by a chain reaction sequence, the overall reaction is not explosive because the process lacks a *chain branching* step commonly seen in hydrocarbon combustion. This will be the topic of a later section.

3.1.6 The Nature of Unimolecular Reactions

The nature of unimolecular reactions may be explained by a chain reaction process. As we discussed before, a unimolecular reaction requires collision to proceed to the products. This is quite obvious since a molecule would not spontaneously dissociate or fragment unless a sufficient amount of energy is placed inside the molecule. For gas-phase reactions, this energy "pumping" process is carried out by collision. It is this same collision process that is responsible for the fact that the rate constant of a unimolecular reaction is sometimes dependent on pressure or total concentration. The underlying mechanism is known as the Lindemann mechanism.

In the Lindemann mechanism, we write a unimolecular reaction in three separate steps:

$$A + M \rightarrow A^* + M \tag{3.27f}$$

$$A^* + M \rightarrow A + M \tag{3.27b}$$

$$A^* \rightarrow \text{products,} \tag{3.28}$$

where M is any gas molecules, and A^* is the reactant capable of overcoming the *potential energy barrier* to form the products. For a simple bond breaking reaction, this energy barrier is equal to the bind dissociation energy (see, Figure 2.8).

The first two steps of the above reaction sequence essentially describe a *collision activation/deactivation* process. That is, molecular collisions lead to constant fluctuations of internal energy in a molecule. The last step represents an energized molecule undergoes spontaneous reaction to form the products.

We may write the reaction rate for A^* as

$$\frac{d\left[A^*\right]}{dt} = k_{27f}[A][M] - \left(k_{27b}[M] + k_{28}\right)\left[A^*\right] . \tag{3.29}$$

Again, since A^* is unstable (that is, a energized molecule would either be de-energized through collision or be destroyed through spontaneous reaction), it cannot accumulate in the reactor. In other words, we may make the steady state assumption for A^*, such that

$$\frac{d\left[A^*\right]_{ss}}{dt} = k_{27f}[A][M] - \left(k_{27b}[M] + k_{28}\right)\left[A^*\right]_{ss} = 0 , \tag{3.30}$$

or

$$\left[A^*\right]_{ss} = \frac{k_{27f}[M]}{\left(k_{27b}[M] + k_{28}\right)}[A] . \tag{3.31}$$

The net rate for the unimolecular reaction (3.1) is therefore

$$-\frac{d[A]}{dt} = k_{28}\left[A^*\right]_{ss} = \frac{k_{28}k_{27f}[M]}{\left(k_{27b}[M] + k_{28}\right)}[A] = \left(\frac{1}{k_{28}\,k_{27f}/k_{27b}} + \frac{1}{k_{27f}[M]}\right)^{-1}[A] . \tag{3.32}$$

The above equation defines the effect rate constant for a unimolecular reaction k_{uni} as

$$k_{uni} = \left(\frac{1}{k_{28}\,k_{27f}/k_{27b}} + \frac{1}{k_{27f}[M]}\right)^{-1} . \tag{3.33}$$

Suppose the reaction is carried out at very low pressure (i.e., $p \to 0$ and $[M] = p/R_uT \to 0$). We have

$$k_{uni,0} = k_{27f}[M] , \tag{3.34}$$

where the subscript denotes the *low-pressure* limit. Here we note that at this low-pressure limit, the rate constant of a unimolecular reaction is proportional to pressure, as discussed in section 3.1.2 and shown in Figure 3.2. Conversely, at the *high-pressure* limit $[M] \to \infty$ and we have

$$k_{uni,\infty} = k_{28}\, k_{27f} / k_{27b} \;, \tag{3.35}$$

which is independent of pressure and is a constant if the temperature is fixed (see, Figure 3.2). The overall pressure dependence of the rate constant of a unimolecular reaction may now be written as

$$\frac{1}{k_{uni}} = \frac{1}{k_{uni,0}} + \frac{1}{k_{uni,\infty}} \;. \tag{3.36}$$

The dependence of k_{uni} as a function of total concentration [*M*] or pressure *p* may be illustrated in Figure 3.2.

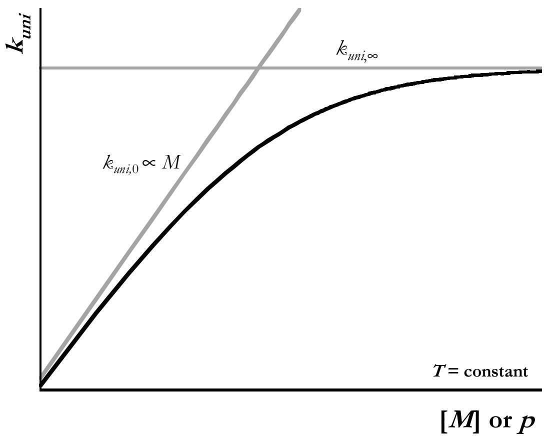

Figure 3.2 The pressure dependence of the rate constant of a unimolecular reaction.

In general, the rate constant of unimolecular reaction of small molecules (e.g., diatomics) tends to be close to the low-pressure limit at the ambient pressure, whereas that of large molecules tends to be in the high-pressure limit. The cause for this will be discussed in Lecture 4.

While the Lindemann mechanism explained the qualitative pressure dependence of the rate constant of a unimolecular reaction, quantitatively it is still very inaccurate. Again we will learn in Lecture 4 some of the more advance theories that can describe unimolecular reactions in a more quantitative manner.

3.1.7 The Arrhenius Law

Reaction rate constants of most reactions are strongly dependent on temperature. This dependency is given by the Arrhenius law as

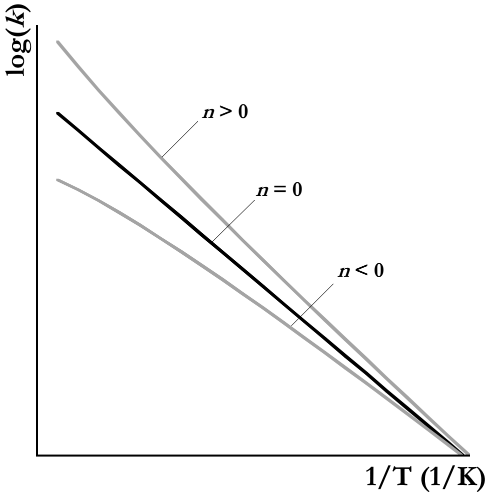

Figure 3.3 Arrhenius plot of rate constant versus 1/*T*.

$$k = A\exp\left(-\frac{E_a}{R_u T}\right) , \tag{3.37}$$

where A is called the pre-exponential factor and E_a (kJ/mol) is the activation energy. The units of A are 1/s, cm^3/mol-s, and cm^6/mol^2-s for unimolecular, bimolecular and termolecular reactions, respectively. Paradoxically the rate constant is not a constant. Rather it depends on temperature. It is for this reason that we shall refer the rate constant as rate coefficient.

In general, the pre-factor A is not a constant. A modified Arrhenius expression may be introduced to account for this effect, i.e.,

$$k = BT^n \exp\left(-\frac{E_a}{R_u T}\right) , \tag{3.38}$$

where B is a constant and n is called the temperature exponent. An Arrhenius plot of log$k$-versus-1/T is usually used to illustrate the temperature dependence, as shown in Figure 3.3.

The strong dependence of k on temperature may be illustrated by examining the following reaction

$$H\bullet \; + \; O_2 \rightarrow O\bullet \; + OH\bullet \; ,$$

with[*]

$$k\left(\text{cm}^3/\text{mol-s}\right) = 2.65\times 10^{16} T^{-0.671} \exp\left[-\frac{71.3\ (\text{kJ/mol})}{R_u T}\right] .$$

---

[*] Taken from Davis, S. G., Joshi, A. V., Wang, H., and Egolfopoulos, F., "An optimized kinetic model of H_2/CO combustion." *Proceedings of the Combustion Institute*, **30**, pp. 1283-1292, 2005.

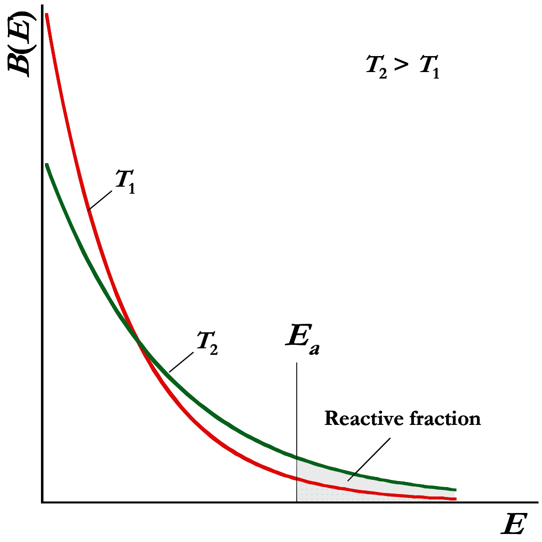

Figure 3.4 Boltzmann distribution of kinetic energy and reactive fractions of molecules.

we may calculate that $k(1200\ \text{K}) = 1.8\times10^{11}$ (cm³/mol-s) and $k(1400\ \text{K}) = 4.5\times10^{11}$ (cm³/mol-s). Therefore a 17% increase in temperature causes a factor of 2.5 increase in the rate coefficient. This strong temperature dependence has its notable impact on a combustion process, as will be discussed later.

3.1.8 The Activation Energy

The origin of the activation energy is the Maxwell-Boltzmann distribution of energy. In the continuous form, we have

$$B(E)=\frac{N_E}{N_{tot}}=\frac{1}{Q}\exp\left(-\frac{E}{k_BT}\right)\ . \tag{3.39}$$

The fraction of molecules having energy greater than the activation energy is given by the shaded area as shown in Figure 3.4. Thus the significance of the activation energy is that it represents the kinetic energy level in a molecule above which the reaction is possible. Because the partition function increases with an increase in temperature, the $B(E)$ curve tends to flatter at higher temperatures. This effectively leads more molecules to possess internal kinetic energies greater than E_a (*cf*, the $B(E)$ curves for T_1 and T_2 with $T_2 > T_1$). In this way, the rate coefficient depends on the temperature in an exponential manner.

3.1.9 Summary and a General Comment about the Pressure and Temperature Dependence of Rate Coefficient

In general, the rate coefficient of a unimolecular reaction is dependent on both temperature and pressure, as discussed in section 3.16. At very low pressures, the rate coefficient is directly proportional to pressure. At very high pressures, the rate coefficient becomes independent of pressure. For bimolecular reactions, the rate coefficients are by and large dependent only on temperature. There are exceptions, but we will leave the discussion to a later time.

3.2 Chemical Reaction Mechanism of Fuel Combustion

Although our knowledge of reaction kinetics remains empirical, this knowledge is nonetheless sufficient for us analyze some typical combustion processes.

The detailed explanation at the molecular level how a reaction proceeds is called *reaction mechanism*. In general, a chemical reaction mechanism is a collection of elementary reactions that describes the fuel oxidation processes, from the beginning to the end. Needless to say, the end state given by the reaction mechanism must be consistent with thermodynamic prediction for the end state of an overall reaction process. Before we begin to discuss the mechanism of fuel oxidation, starting from hydrogen (H_2), we wish to diverge a bit by discussing the invention of the chess game and the nature of exponential growth. The purpose of this discussion will soon become clear.

3.2.1 Chess

Legend says that the game of chess was invented by Grand Vizier Sissa Ben Dahir, who presented it to King Shirham of India as a gift. In gratitude, the king offered the Grand Visir any reward requested, provided, of course, that it sounded reasonable.

The Grand Vizier asked for only:

"One grain of wheat, representing the first square of a chessboard. Two grains for the second square. Four grains for the next. Then eight, sixteen, thirty two … doubling for each successive square until the 64*th* and last square is counted."

The king was impressed with the apparent modesty of the request, and he immediately granted it. He took his chess board, removed the pieces, and asked for a bag of wheat to be brought in. But, to his surprise, the bag was emptied by the 20th square. The king had another bag brought in, but then realized that the entire second bag was needed for just the next square. In fact, in 20 more squares, he would need as many bags as there were grains of wheat in the first bag!

The number of grains for the last square can be calculated as 2^{63} or 9.22×10^{18}. If you include the grains on the first 63 squares, the sum is about twice as large, $\sim2\times10^{19}$. If each grain were spherical 1 mm in diameter, then the volume would be about 10 km^3. If the grain were staked in a square 1 m in height, it would occupy a land 10^5 km^2 in area, which is far more than what the kingdom ever possesses or would ever be able to produce.

Legend does not record what the king did to his Grand Vizier.

The amazing feature of this problem is that with just 63 steps, each one quite modest, you get a huge number at the end. This type of rapid growth is called exponential growth. Exponential growth is the secret behind a large number of combustion phenomena we

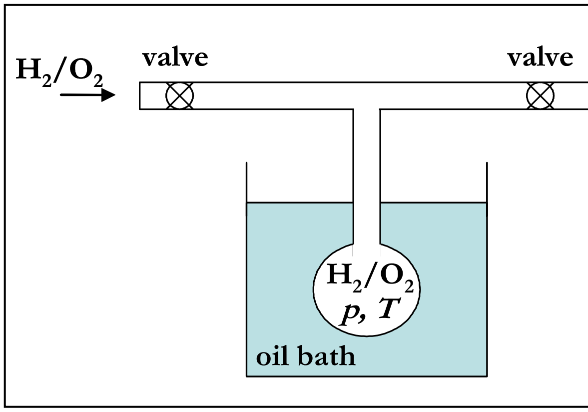

Figure 3.5 Schematic illustration of experimental measurements of hydrogen explosion.

discuss in this section. Here the reactive free radicals generated in a reaction process are analogous to the grains in Grand Visir's mathematical game.

3.2.1 The Explosion Limits of Hydrogen

Consider an experiment in which a reactor is completely immersed in an oil bath at temperature *T* (see, Figure 3.5). The reactor is fed continuously with a fresh, reactant mixture of hydrogen (H_2) and oxygen (O_2). Under a steady flow of the reactant mixture, the pressure inside the reactor may be controlled by adjusting the two valves. Holding the temperature constant while increasing the pressure may lead to an explosion in the reactor that may be easily observed, since the reaction rate increases with an increase in pressure or species concentration.

The actual experiments show that the situation is far more complicated. Figure 3.6 illustrates the complex dependence of pressure at which explosion may be observed as a function of temperature. Specifically we observe a zig-zag curve that separates the non-explosive (p, T) regime from the explosive regime. The three branches of the p-T curves are called the first, the second and the third explosion limits.

Let us explain the first and second explosion limits first. The initiation of the free radical chain reaction in a mixture of hydrogen and oxygen starts from

$$H_2 + O_2 \rightarrow H\bullet + HO_2\bullet\ . \qquad \text{(chain initiation)} \qquad (3.40)$$

The resulting $H\bullet$ atom will attack the reactant O_2 through

$$H\bullet + \mathrm{O_2} \rightarrow O\bullet + OH\bullet\ , \qquad \text{(chain branching)} \qquad (3.41)$$

followed by the products of the above reaction to attack the fuel,

$$O\bullet + \mathrm{H_2} \rightarrow OH\bullet + H\bullet \qquad \text{(chain branching)} \qquad (3.42)$$

$$OH\bullet + \mathrm{H_2} \rightarrow H_2O + H\bullet\ . \qquad \text{(chain propagation)} \qquad (3.43)$$

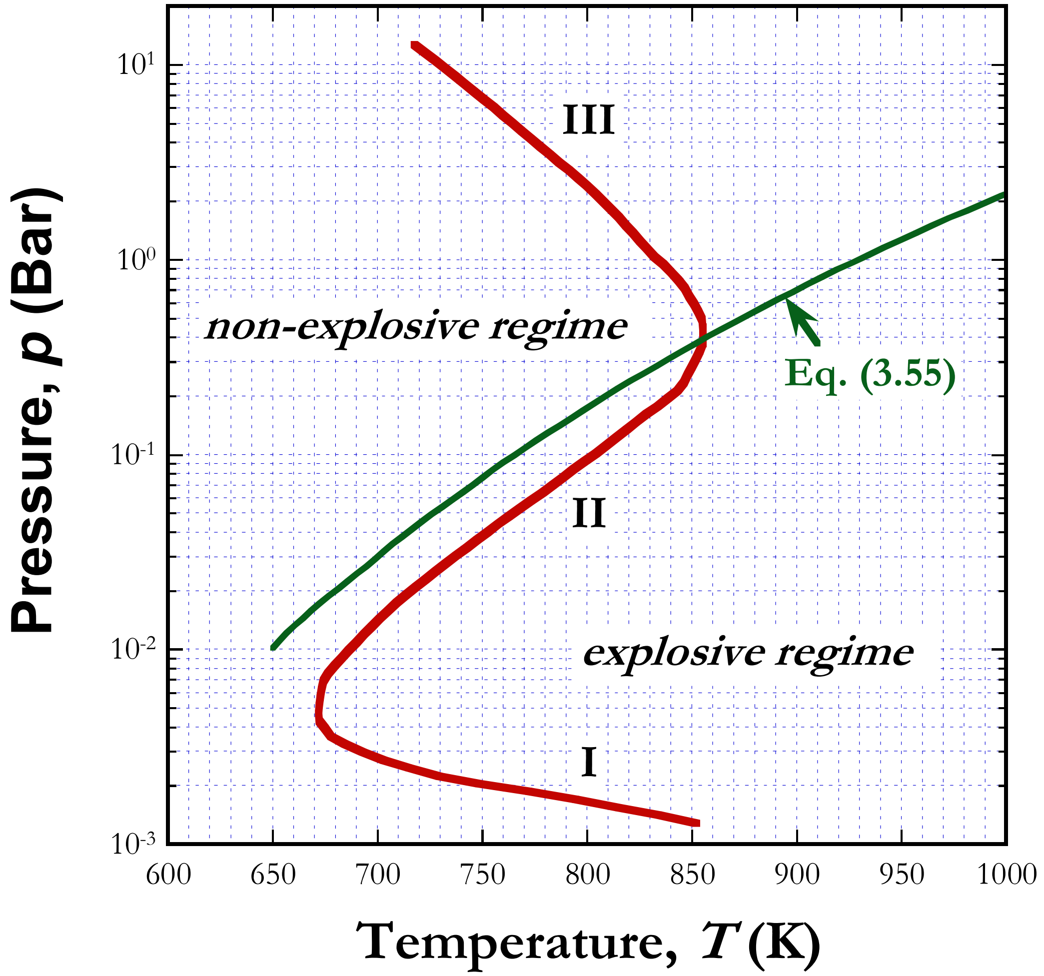

Figure 3.6 Explosion limits of hydrogen.

We see that starting from one $H\bullet$ atom, one cycle of chain reaction led to the production of 3 $H\bullet$ atoms. Note that steps 3.41 and 3.42 collectively generate two OH• radicals, which form 2 $H\bullet$ atoms through 3.43. The third $H\bullet$ atom is produced from step 3.43. The three $H\bullet$ atoms then undergo another cycle of reaction to generate 9, 27 and 81 $H\bullet$ atoms and so on. Therefore the way how the number of free radicals triples is similar to Grand Visir's chess-board game. As will be discussed in later sections, reaction (3.41) is by far the most important chain branching reaction in hydrocarbon combustion.

Reactions (3.41) and (3.42) are termed the *chain branching* reactions, since the reactions of one reactive, free radical yield two free radicals. Unlike the reaction between H_2 and Br_2 (section 3.1.4), in which the overall rate of reaction depends on the chain initiation rate, the reaction of H_2 and O_2 is not too dependent on the rate of chain initiation, since the number of radicals quickly multiply in the chain reaction sequence. This type of chain reactions is called the branched chain reactions.

Note that in each chain cycle, one water molecule is produced. Since the production of water is associated with the release of a given amount of energy, the faster and faster branched chain reaction process causes the rate of heat release to increase exponentially, to the point that the heat generated cannot be removed faster enough from the reactor. Explosion occurs.

If the aforementioned mechanism is true, why would we see a zig-zag p-T curves? There are several reasons here. The main chain termination reactions in H_2 oxidation are

$$H\bullet \rightarrow \text{wall destruction} \qquad \text{(chain termination)} \qquad (3.44)$$
$$H\bullet + O_2 + M \rightarrow HO_2\bullet + M \qquad \text{(chain termination)} \qquad (3.45)$$
$$HO_2\bullet + HO_2\bullet + M \rightarrow H_2O_2 + O_2 + M \qquad \text{(chain termination)} \qquad (3.46)$$

where the $HO_2\bullet$ is the hydrogen peroxy radical and H_2O_2 is hydrogen peroxide. Reaction (3.44) is governed by the diffusion of the $H\bullet$ atom to the reactor wall. The rate of diffusion is inversely proportional to pressure, a topic we will discuss sometime later. At very low pressure ($< 10^{-2}$ Bar), diffusional wall loss is the dominant chain termination step. For this reason, the H_2/O_2 mixture cannot explode since all $H\bullet$ atoms produced from the chain initiation (4.40) quickly diffuse to the wall and destructed on the wall. As the pressure is increased, the diffusion rate decreases. Some of the $H\bullet$ atoms now would react through reactions (3.41-43) to cause explosion. This explains the first explosion limit.

The second explosion limit is peculiar in that as the pressure is further raised inside the peninsular of the explosion regime, the mixture becomes nonexplosive again. The cause for the second explosion limit may be understood by considering the pressure dependence of the chain termination step (3.45). Since $[M]$ is proportional to p, an increase in pressure causes more $H\bullet$ atoms to react and form the relatively non-reactive hydrogen peroxy radical $HO_2\bullet$, which are destroyed by the wall or through reaction (3.46). In this way, the termination reaction (3.45) competes more effectively with the chain branching reaction (3.41) as pressure is increased. Eventually the branching reaction loses completely to the termination step. The system reactivity drops to zero and the reactant mixture becomes non-explosive again.

The second explosion limit may be mathematically modeled by the handful of reactions described above. Specifically, we write the rate of $H\bullet$, $O\bullet$, and $OH\bullet$ production as

$$\frac{d[H\bullet]}{dt} = -k_{41}[H\bullet][O_2] + k_{42}[O\bullet][H_2] + k_{43}[OH\bullet][H_2] - k_{45}[H\bullet][O_2][M] \ , \qquad (3.47)$$

$$\frac{d[O\bullet]}{dt} = k_{41}[H\bullet][O_2] - k_{42}[O\bullet][H_2] \ , \qquad (3.48)$$

$$\frac{d[OH\bullet]}{dt} = k_{41}[H\bullet][O_2] + k_{42}[O\bullet][H_2] - k_{43}[OH\bullet][H_2] \ . \qquad (3.49)$$

Here we neglect the initiation reaction since its rate is small. Since the O• and *OH*• radicals are extremely reactive, we make the assumption that their concentration is in a steady state. It may be shown that a combination of Eqs. (3.47-49) gives

$$\frac{d[H\bullet]}{dt} = 2k_{41}[H\bullet][O_2] - k_{45}[H\bullet][O_2][M] \ , \tag{3.50}$$

Since for mixture to explode we need a net accumulation of H• atoms, we have

$$2k_{41}[H\bullet][O_2] - k_{45}[H\bullet][O_2][M] \begin{cases} < 0 & \text{no explosive} \\ = 0 & \text{explosion limit} \\ > 0 & \text{explosive} \end{cases} . \tag{3.51}$$

It follows that the second explosion limit is given by

$$[M] = \frac{p}{R_u T} = 2\frac{k_{41}}{k_{45}} \ . \tag{3.52}$$

Using*

$$k_{41}\left(\text{cm}^3/\text{mol-s}\right) = 2.65\times10^{16} T^{-0.671} \exp\left[-\frac{71.3\ (\text{kJ/mol})}{R_u T}\right] \tag{3.53}$$

$$k_{45}\left(\text{cm}^6/\text{mol}^2\text{-s}\right) = 4.31\times10^{19} T^{-1.4} \tag{3.54}$$

we obtain

$$p(\text{atm}) = 0.1T^{1.729} e^{-8576/T} \ . \tag{3.55}$$

Here we note that for k_{45}, we have chosen the rate expression for $M = O_2$. The simple analysis presented above gives a calculated, second explosion boundary in semi-quantitative agreement with the experiment (see, Figure 3.6). Though the result is not exact, it nonetheless demonstrates that overall trend is correct. More importantly, this exercise illustrates the need to understand detailed chain *branching*, *propagation*, and *termination* in order to explain the phenomena of fuel explosion, even for the simplest fuel – hydrogen.

In the third explosion limit, the reactant mixture becomes explosive again as the pressure is increased. The origin for enhanced reactivity is the reactions of hydrogen peroxy radical *HO*₂•. Though it is only mildly reactive, a great accumulation of this species in the reactor does cause intense heat release through a different chain reaction mechanism:

$H\bullet + O_2 + M \rightarrow HO_2\bullet + M$ (chain propagation) (3.45)
$HO_2\bullet + HO_2\bullet \rightarrow H_2O_2 + O_2$ (chain termination) (3.46)

$H_2O_2 + M \rightarrow OH\bullet + OH\bullet + M$ (chain branching) (3.56)
$OH\bullet + H_2 \rightarrow H_2O + H\bullet$ (chain propagation) (3.43)
$H\bullet + HO_2\bullet \rightarrow OH\bullet + OH\bullet$ (chain propagation) (3.57)
$H\bullet + HO_2\bullet \rightarrow H_2 + O_2$ (chain termination) (3.58)
$OH\bullet + HO_2\bullet \rightarrow H_2O + O_2\,.$ (chain termination) (3.59)

Here reaction (3.45) becomes a chain propagation step, instead of chain terminating, since the resulting $HO_2\bullet$ radicals undergoes self reaction to form H_2O_2. Although the latter reaction seems to be chain terminating, the rapid dissociation (3.56) of its product, H_2O_2, causes effective chain branching, and as such the steps combining (3.45, 3.46 and 3.56) represent a straight chain process, without effective branching or termination.

A detailed reaction mechanism of H_2 combustion over all range of conditions is a bit more involved. Figure 3.7 illustrates an example of this reaction mechanism. In addition to the parameters of the modified Arrhenius equation ($A = B$, n, E), there are several other terms appeared in the figure. These will be discussed later.

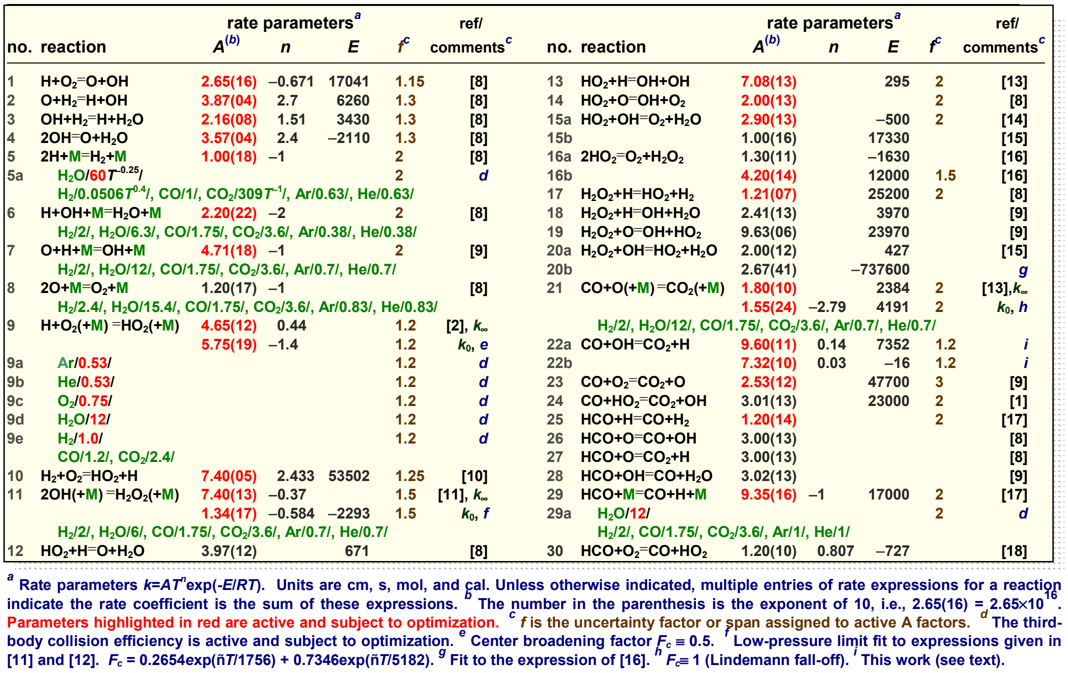

		rate parameters[a]				ref/
no.	reaction	$A^{(b)}$	n	E	f^c	comments[c]
1	$H+O_2=O+OH$	2.65(16)	–0.671	17041	1.15	[8]
2	$O+H_2=H+OH$	3.87(04)	2.7	6260	1.3	[8]
3	$OH+H_2=H+H_2O$	2.16(08)	1.51	3430	1.3	[8]
4	$2OH=O+H_2O$	3.57(04)	2.4	–2110	1.3	[8]
5	$2H+M=H_2+M$	1.00(18)	–1		2	[8]
5a	$H_2O/60T^{-0.25}/$				2	*d*
	$H_2/0.0506T^{0.4}/$, $CO/1/$, $CO_2/309T^{-1}/$, $Ar/0.63/$, $He/0.63/$					
6	$H+OH+M=H_2O+M$	2.20(22)	–2		2	[8]
	$H_2/2/$, $H_2O/6.3/$, $CO/1.75/$, $CO_2/3.6/$, $Ar/0.38/$, $He/0.38/$					
7	$O+H+M=OH+M$	4.71(18)	–1		2	[9]
	$H_2/2/$, $H_2O/12/$, $CO/1.75/$, $CO_2/3.6/$, $Ar/0.7/$, $He/0.7/$					
8	$2O+M=O_2+M$	1.20(17)	–1			[8]
	$H_2/2.4/$, $H_2O/15.4/$, $CO/1.75/$, $CO_2/3.6/$, $Ar/0.83/$, $He/0.83/$					
9	$H+O_2(+M)=HO_2(+M)$	4.65(12)	0.44		1.2	[2], k_∞
		5.75(19)	–1.4		1.2	k_0, *e*
9a	$Ar/0.53/$				1.2	*d*
9b	$He/0.53/$				1.2	*d*
9c	$O_2/0.75/$				1.2	*d*
9d	$H_2O/12/$				1.2	*d*
9e	$H_2/1.0/$				1.2	*d*
	$CO/1.2/$, $CO_2/2.4/$					
10	$H_2+O_2=HO_2+H$	7.40(05)	2.433	53502	1.25	[10]
11	$2OH(+M)=H_2O_2(+M)$	7.40(13)	–0.37		1.5	[11], k_∞
		1.34(17)	–0.584	–2293	1.5	k_0, *f*
	$H_2/2/$, $H_2O/6/$, $CO/1.75/$, $CO_2/3.6/$, $Ar/0.7/$, $He/0.7/$					
12	$HO_2+H=O+H_2O$	3.97(12)		671		[8]
13	$HO_2+H=OH+OH$	7.08(13)		295	2	[13]
14	$HO_2+O=OH+O_2$	2.00(13)			2	[8]
15a	$HO_2+OH=O_2+H_2O$	2.90(13)		–500	2	[14]
15b		1.00(16)		17330		[15]
16a	$2HO_2=O_2+H_2O_2$	1.30(11)		–1630		[16]
16b		4.20(14)		12000	1.5	[16]
17	$H_2O_2+H=HO_2+H_2$	1.21(07)		25200	2	[8]
18	$H_2O_2+H=OH+H_2O$	2.41(13)		3970		[9]
19	$H_2O_2+O=OH+HO_2$	9.63(06)		23970		[9]
20a	$H_2O_2+OH=HO_2+H_2O$	2.00(12)		427		[15]
20b		2.67(41)		–737600		*g*
21	$CO+O(+M)=CO_2(+M)$	1.80(10)		2384	2	[13], k_∞
		1.55(24)	–2.79	4191	2	k_0, *h*
	$H_2/2/$, $H_2O/12/$, $CO/1.75/$, $CO_2/3.6/$, $Ar/0.7/$, $He/0.7/$					
22a	$CO+OH=CO_2+H$	9.60(11)	0.14	7352	1.2	*i*
22b		7.32(10)	0.03	–16	1.2	*i*
23	$CO+O_2=CO_2+O$	2.53(12)		47700	3	[9]
24	$CO+HO_2=CO_2+OH$	3.01(13)		23000	2	[1]
25	$HCO+H=CO+H_2$	1.20(14)			2	[17]
26	$HCO+O=CO+OH$	3.00(13)				[8]
27	$HCO+O=CO_2+H$	3.00(13)				[8]
28	$HCO+OH=CO+H_2O$	3.02(13)				[9]
29	$HCO+M=CO+H+M$	9.35(16)	–1	17000	2	[17]
29a	$H_2O/12/$				2	*d*
	$H_2/2/$, $CO/1.75/$, $CO_2/3.6/$, $Ar/1/$, $He/1/$					
30	$HCO+O_2=CO+HO_2$	1.20(10)	0.807	–727		[18]

[a] Rate parameters $k=AT^n\exp(-E/RT)$. Units are cm, s, mol, and cal. Unless otherwise indicated, multiple entries of rate expressions for a reaction indicate the rate coefficient is the sum of these expressions. [b] The number in the parenthesis is the exponent of 10, i.e., 2.65(16) = 2.65×10^{16}. Parameters highlighted in red are active and subject to optimization. [c] *f* is the uncertainty factor or span assigned to active A factors. [d] The third-body collision efficiency is active and subject to optimization. [e] Center broadening factor $F_c \equiv 0.5$. [f] Low-pressure limit fit to expressions given in [11] and [12]. F_c = 0.2654exp(ñ*T*/1756) + 0.7346exp(ñ*T*/5182). [g] Fit to the expression of [16]. [h] $F_c \equiv 1$ (Lindemann fall-off). [i] This work (see text).

Figure 3.7 A detailed reaction mechanism of H_2/CO oxidation at high temperatures (adapted from Davis, S. G., Joshi, A. V., Wang, H., and Egolfopoulos, F., "An optimized kinetic model of H_2/CO combustion." *Proceedings of the Combustion Institute*, **30**, pp. 1283-1292, 2005).

In flames burning hydrogen as a fuel, the reaction mechanism is similar to those that have already been discussed.

3.2.2 The Oxidation of Carbon Monoxide

Pure and dry carbon monoxide is difficult to burn. The principal cause is that there lacks a free radical chain branching and propagation mechanism to facilitate continuous and accelerated CO conversion to CO_2. Here the reaction steps may be postulated as

$$CO + O_2 \rightarrow CO_2 + O\bullet \qquad \text{(chain initiation)} \qquad (3.60)$$
$$CO + O\bullet + M \rightarrow CO_2 + M\,. \qquad \text{(chain termination)} \qquad (3.61)$$

In early studies, a vast number of CO oxidation data appeared to be difficult to reconcile amongst themselves. It was realized later that a trace amount of water, resulting from the impurity in CO or moisture brought by air can notably affect the oxidation rates of carbon monoxide. The explanation lies in the hydrogen brought by water. Specifically, in the presence of water we have the following sequence of reactions:

$$CO + O_2 \rightarrow CO_2 + O\bullet \qquad \text{(chain initiation)} \qquad (3.60)$$
$$O\bullet + H_2O \rightarrow OH\bullet + OH\bullet \qquad (3.61)$$
$$CO + OH\bullet \rightarrow CO_2 + H\bullet \qquad \text{(chain propagation)} \qquad (3.62)$$
$$H\bullet + O_2 \rightarrow O\bullet + OH\bullet\,, \qquad \text{(chain branching)} \qquad (3.41)$$

Notice that the trace amount of water essentially supplies the $H\bullet$ otherwise not available in dry CO oxidation. In this way, the conversion of CO to CO_2 is now catalyzed by the $OH\bullet$ radical (3.62) and by the chain branching reaction (3.41). If H_2 is present, the reactions

$$O\bullet + H_2 \rightarrow OH\bullet + H\bullet \qquad \text{(chain branching)} \qquad (3.42)$$
$$OH\bullet + H_2 \rightarrow H_2O + H\bullet\,. \qquad \text{(chain propagation)} \qquad (3.43)$$

will participate in the chain reaction process, again with $H\bullet$ production to be crucial to the overall oxidation rates.

The oxidation of CO is in fact always dominated by reaction (3.62) so long as hydrogen, molecular or atomic, is available in the combustor. Aside from the fact that (3.62) produces the much needed $H\bullet$ atoms to facilitate chain branching and that it serves to convert most of the CO to the final combustion product CO_2, it also releases a large amount of heat, i.e., $\Delta H^{\circ}_{r,298.15K} = -104$ kJ/mol. As will be discussed in the next few sections, reaction (3.62) is the second most important reaction in hydrocarbon combustion, since hydrogen is always abundantly available in hydrocarbon fuels.

3.2.3 Explosion Limits of Hydrocarbons

Figure 3.8 shows the lines that separate the explosive and non-explosive regimes for methane, ethane, and propane. There several important features here. First, the explosion pressure generally decreases with an increase in temperature. It is expected since the reaction rates and reactivity increases with increases in both pressure and temperature. Therefore, decreases of reactivity resulting from a lower temperature may be compensated

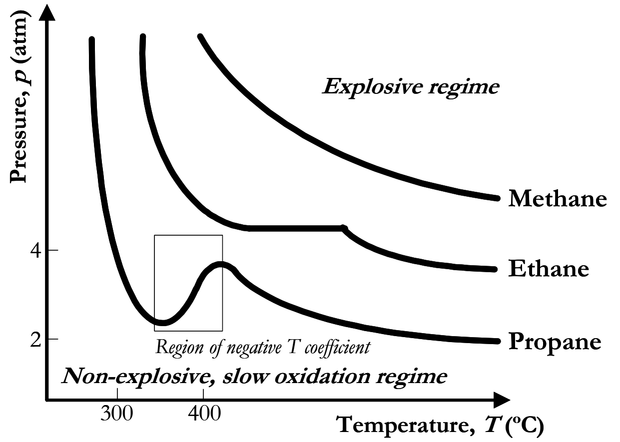

Figure 3.8. Explosion limits of methane, ethane and propane.

by an increase in reactor pressure, and as a general rule of thumb, the explosion *p*-*T* curves are monotonic decay functions. Second, it is more difficult for methane to undergo explosion then ethane, and the explosion of ethane is more difficult that propane and higher alkane hydrocarbons. This order is consistent with the order of C-H bond dissociation energies (strengths) of methane (439 kJ/mol), ethane (420 kJ/mol) and propane (413 kJ/mol). In other words, the larger strength of the C-H bond energy in methane makes it more difficult to break the bond to allow for free-radical chain reactions.

For higher alkanes, such as propane, some complications arise in the explosion *p*-*T* curve, as seen in Figure 3.8. Specifically, we observe that in a particular *p*-*T* region, an increase in temperature is accompanied with an increased explosion pressure. In other words, an increase in temperature in this region actually caused a lowered reactivity. This region is known as the *negative temperature-coefficient* (NTC) region.

To understand the NTC behavior, we need to digress here and re-visit the hydrogen explosion limits. Recall that the second explosion limit is dictated by the chain branching reaction (3.41)

$$H\bullet + \mathrm{O_2} \rightarrow O\bullet + OH\bullet\,, \qquad \text{(chain branching)} \qquad (3.41)$$

and chain termination reaction (2.45)

$$H\bullet + \mathrm{O_2} + M \rightarrow HO_2\bullet + M \qquad \text{(chain termination)} \qquad (3.45)$$

If we extrapolate the second-explosion limit curve to high temperatures, we found that to achieve explosive reactivity at ~1 atm, i.e., where the reaction (2.41) becomes faster than (2.45), the breaking point in temperature is around 1000 K. At higher pressures, this dividing temperature is expected to be higher.

Note that for propane the NTC region occurs in the temperature range of 300 – 400 ºC or ~550 – 650 K, far below the temperature one would expect to see a chain branching process dominated by (3.41). Therefore some other reaction mechanisms must be responsible for the intricate explosion behavior of propane. To help us to understand this mechanism, we shall start our discussion with methane oxidation far below the temperature of $H\bullet$ + O_2 chain branching.

3.2.4 Low-Temperature Methane Oxidation Chemistry

Compared with the bond energy in H_2 (435 kJ/mol), the C-H bond energy in methane is 439 kJ/mol (see, Table 2.2). Therefore, like hydrogen oxidation, the free-radical chain initiation in methane is accomplished by the abstraction of H• atom by O_2

$$CH_4 + O_2 \rightarrow CH_3\bullet + HO_2\bullet\ . \qquad (3.63)$$

At the moderate pressure of 1 to 10 atm and if the temperature is sufficiently low (< 800 K), the dominant reaction that follows would be the addition of O_2 to the methyl radical,

$$CH_3\bullet + O_2\ (+M) \rightarrow CH_3O_2\bullet\ (+M)^{\dagger}\ . \qquad (3.64)$$

This is followed by H-abstraction from methane by the methyl peroxy radical $CH_3O_2\bullet$, i.e.,

$$CH_4 + CH_3O_2\bullet \rightarrow CH_3O_2H + CH_3\bullet. \qquad (3.65)$$

Chain branching is accomplished with the dissociation of methyl peroxide CH_3O_2H, i.e.,

$$CH_3O_2H\ (+M) \rightarrow CH_3O\bullet + OH\bullet\ (+M) \qquad (3.66)$$

Several chain propagation reactions follow, due to the dissociated products of (3.66),

$$CH_3O\bullet + O_2 \rightarrow CH_2O + HO_2\bullet \qquad (3.67)$$
$$CH_4 + OH\bullet \rightarrow CH_3\bullet + H_2O \qquad (3.68)$$
$$CH_3O_2H + OH\bullet \rightarrow CH_3O_2\bullet + H_2O \qquad (3.69)$$

Obviously the above chain reaction mechanism requires reaction (3.64) to proceed in the forward direction and produce the $CH_3O_2\bullet$ radical.

Again, bond formation is favored from the standpoint of enthalpy, but it is not favored by entropy considerations. An increase in temperature causes the $T\Delta S_r^\circ$ term to become more and more negative, and as such the entropy term becomes more competitive to push the reaction in the direction of dissociation or bond breaking, rather than bond formation.

Although the reaction (3.64) is exothermic $\Delta H^\circ_{r,298.15K} = -119$ kJ/mol (almost independent of temperature in the range of 298.15 and 1000 K), its exothermicity is not large enough to

---

[†] Notice that we used the (+*M*) symbol to denote that the rate constant of the above reaction may or may not depend on pressure. In general, as the molecule becomes larger the rate constant of a unimolecular dissociation or a bimolecular combination reaction becomes less pressure sensitive. The cause of this will be clear when we discuss more advanced theories of unimolecular reaction.

hold the C-O bond in the $CH_3O_2\bullet$ radical together at high temperature. Consider the entropy of reaction, $\Delta S^\circ_{r,298.15K} = -137$ J/mol-K (again, nearly a constant over the 298.15 to 1000 K range). We may calculate the Gibbs function change of reaction (3.64) to be $\Delta G^\circ_r \cong$ –78, –8 and 18 kJ/mol at 298.15, 800 and 1000 K, respectively.

Recall that in our discussion of chemical equilibrium, we stated that the Gibbs function must decrease in order for a reaction to proceed forward. Notice that ΔG°_r changes its sign and becomes positive around 800 K. Obviously, this means that reaction (3.64) will reverse itself; and the $CH_3O_2\bullet$ concentration should decrease rapidly as temperature becomes higher. Quantitatively, we may calculate the corresponding equilibrium constant

$$K_p = \frac{[CH_3O_2\bullet]_{eq}}{[CH_3\bullet]_{eq}[O_2]_{eq}}\left(R_u T\right)^{-1} = e^{-\Delta G^\circ_r/R_u T} \tag{3.70}$$

to be approximately 5×10^{13}, 3 and 0.1 (atm^{-1}) at 298.15, 800 and 1000 K, respectively. Take, for example, T = 800 K and p = 1 atm. *We* have $[CH_3O_2\bullet]_{eq}/[CH_3\bullet]_{eq}[O_2]_{eq} = 3\times R_u T$ = 2.1×10^5 cm³/mol. If the O_2 mole fraction is 0.2, its molar concentration is 3×10^6 mol/cm³. The equilibrium ratio $[CH_3O_2\bullet]_{eq}/[CH_3\bullet]_{eq} \cong 0.6$. At 1000 K, however, this ratio drops to ~0.02.

In addition to the thermodynamic reason, the rate coefficient of reaction (3.64) also drops very rapidly. For example, the three-body rate coefficient of

$$CH_3\bullet + O_2 + M \rightarrow CH_3O_2\bullet + M, \tag{3.64a}$$

is quoted to be[‡]

$$k_{64a}\ (\mathrm{cm^6/mol^2\text{-}s}) = 3.7\times10^{17}\ (T/298)^{-3.3} \quad \text{for } 300 \le T\ (\mathrm{K}) \le 800.$$

The combined considerations of reaction thermodynamics and kinetics therefore suggest that the aforementioned reaction mechanism is important only to methane oxidation at temperatures below ~800 K. This mechanism is often termed the *low-temperature* chemistry of methane oxidation.

3.2.5 Methane Oxidation in the Intermediate Temperature Range

At somewhat higher temperature (>~800 K), the prevailing reaction mechanism of methane oxidation switches to the H_2O_2 chemistry, somewhat similar to the chemistry for the third explosion limit of H_2/O_2. The initiation of free radical chain reaction is again caused by

$$CH_4 + O_2 \rightarrow CH_3\bullet + HO_2\bullet\,. \tag{3.63}$$

[‡] Baulch, D.L.; Cobos, C.J.; Cox, R.A.; Esser, C.; Frank, P.; Just, Th.; Kerr, J.A.; Pilling, M.J.; Troe, J.; Walker, R.W.; Warnatz, J. "Evaluated kinetic data for combustion modeling," J. Phys. Chem. Ref. Data, vol. 21, 411 – 429 (1992).

Subsequent reactions involve mostly the $HO_2\bullet$ and $OH\bullet$ radicals, which sequentially oxide methane to formaldehyde (CH_2O), followed by CO and CO_2,

$$CH_4 + OH\bullet \rightarrow CH_3\bullet + H_2O \tag{3.71}$$
$$CH_3\bullet + O_2 \rightarrow CH_2O + OH\bullet \tag{3.72}$$
$$CH_3\bullet + HO_2\bullet \rightarrow CH_3O\bullet + OH\bullet \tag{3.73}$$
$$CH_3O\bullet + O_2 \rightarrow CH_2O + HO_2\bullet \tag{3.74}$$
$$CH_2O + OH\bullet \rightarrow HCO\bullet + H_2O \tag{3.75}$$
$$HCO\bullet + O_2 \rightarrow CO + HO_2\bullet \tag{3.76}$$
$$CO + OH\bullet \rightarrow CO_2 + H\bullet\,. \tag{3.62}$$

In the above chain reaction sequence, the source of $OH\bullet$ is mainly

$$HO_2\bullet + HO_2\bullet \rightarrow H_2O_2 + O_2 \tag{3.46}$$
$$H_2O_2 + M \rightarrow OH\bullet + OH\bullet + M\,, \tag{3.56}$$

where the $HO_2\bullet$ radical comes from

$$H\bullet + O_2 + M \rightarrow HO_2\bullet + M\,. \tag{3.45}$$

The aforementioned reaction sequence is, therefore, dictated by the production of $OH\bullet$ radicals from reactions (3.46) and (3.56), i.e., the same reaction that causes the third explosion limit of hydrogen. For these reactions to take place at appreciable rates, the production of the $HO_2\bullet$ radical from reaction (3.45) must remain to be rapid. This condition, however, deteriorates towards high temperatures.

Figure 3.9 shows the Arrhenius plot for the rate coefficients of reaction (3.45) at several pressures and the chain branching reaction

$$H\bullet + O_2 \rightarrow O\bullet + OH\bullet\,. \tag{3.41}$$

Since we plot $k_{45}[M]$, the comparison shows the relative importance of (3.41) and (3.45) as a function of temperature and pressure. For $p = 1$ atm, the temperature at which the two rate coefficients cross is about 1000 K. At temperatures above this value, the production of $OH\bullet$ would be dominated by (3.41), and not through $HO_2\bullet$. Customarily, the chemistry occurring in the temperature range from about ~800 to 1000 K is termed the *intermediate-temperature* chemistry, where the reactions involving $HO_2\bullet$ and H_2O_2 are responsible to keep the chain reaction going in methane oxidation.

3.2.6 Methane Oxidation in High Temperatures

At temperatures above 1000 K, the dominance of reaction (3.41) brings in another set of chemistry, customarily called the *high temperature* chemistry. The free radicals that carry the chain reactions are $H\bullet$, $O\bullet$, and $OH\bullet$ with some contribution from $HO_2\bullet$. The sequence of chain reaction shares many similarities with the reactions occurred for the intermediate temperature chemistry already discussed.

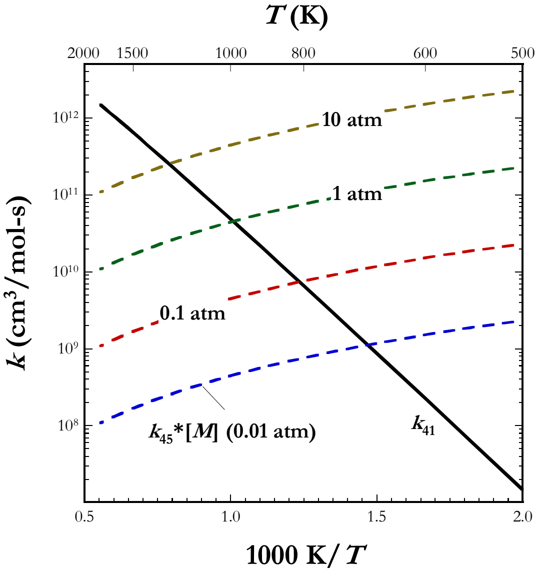

Figure 3.9 Arrhenius plot of k_{41} and $k_{45}[M]$ at several pressures.

The initiation of free radical chain reaction is accomplished through

$$CH_4 + O_2 \rightarrow CH_3\bullet + HO_2\bullet\ , \tag{3.63}$$

but at very high temperature the C-H bond breaking (or fission) in methane can be very important,

$$CH_4\ (+M) \rightarrow CH_3\bullet + H\bullet\ (+M), \tag{3.77}$$

The relative importance of the above two reactions depends on pressure and temperature. The activation energies of the above two reactions are approximately $E_{a,3.63}$ = 234 and $E_{a,3.77}$ = 439 kJ/mol. Because of the large activation energy and the inherent pressure dependence of $k_{3.77}$, this bond fission reaction is favored only at high temperature and high pressure conditions.

The destruction of methane is accomplished by

$$CH_4 + H\bullet \rightarrow CH_3\bullet + H_2 \tag{3.78}$$
$$CH_4 + O\bullet \rightarrow CH_3\bullet + OH\bullet \tag{3.79}$$
$$CH_4 + OH\bullet \rightarrow CH_3\bullet + H_2O\ . \tag{3.71}$$

Depending on the concentration of free radicals in the reactor (i.e., abundant in flames and less abundant prior to explosion or fuel ignition), the dominant reactions of the methyl radicals vary from (less abundant)

$$CH_3\bullet + O_2 \rightarrow CH_2O + OH\bullet \tag{3.72}$$

$$CH_3\bullet + O_2 \rightarrow CH_3O\bullet + O\bullet \tag{3.80}$$
$$CH_3O\bullet + O_2 \rightarrow CH_2O + HO_2\bullet \tag{3.74}$$
$$CH_3O\bullet\ (+M) \rightarrow CH_2O + H\bullet\ (+M) \tag{3.81}$$
$$CH_3\bullet + HO_2\bullet \rightarrow CH_3O\bullet + OH\bullet \tag{3.73}$$

to (abundant)

$$CH_3\bullet + O\bullet \rightarrow CH_2O + H\bullet \tag{3.82}$$
$$CH_3\bullet + OH\bullet \rightarrow CH_2\bullet + H_2O \tag{3.83}$$
$$CH_2\bullet + O_2 \rightarrow HCO\bullet + OH\bullet\ . \tag{3.84}$$
$$CH_3\bullet + HO_2\bullet \rightarrow CH_3O\bullet + OH\bullet\ . \tag{3.73}$$

The destruction of CH_2O proceeds through

$$CH_2O + H\bullet \rightarrow HCO\bullet + H_2 \tag{3.85}$$
$$CH_2O + O\bullet \rightarrow HCO\bullet + OH\bullet \tag{3.86}$$
$$CH_2\mathrm{O} + OH\bullet \rightarrow HCO\bullet + H_2O \tag{3.75}$$
$$HCO\bullet + O_2 \rightarrow CO + HO_2\bullet \tag{3.76}$$
$$HCO\bullet\ (+M) \rightarrow CO + H\bullet\ (+M)\ , \tag{3.87}$$

and finally,

$$CO + OH\bullet \rightarrow CO_2 + H\bullet\ . \tag{3.62}$$

Again the chain branching reaction

$$H\bullet + \mathrm{O}_2 \rightarrow O\bullet + OH\bullet\ . \tag{3.41}$$

is responsible for the explosive, branched chain behavior for methane oxidation at high temperature.

It is clear from the above discussion that the chemistry of C/H/O fuels can get annoyingly complex as the size of the fuel molecule becomes big. There are several important features that are similar among different fuels,

(a) All reaction mechanisms discussed so far involve a chain reaction sequence, though the details of reactions depend on the temperature, pressure, and the nature of the fuel molecule;

(b) For methane oxidation, we see that there are three different sets of chemistry depending on the temperature and pressure. For $T <$ ~800 K, the chain reaction process requires the methyl peroxide intermediate CH_3O_2H to dissociate into two free radicals (3.66). For ~800 $< T <$ 1000 K, the dissociation of hydrogen peroxide H_2O_2 (3.56) is responsible to carry the chain reaction forward. At high temperatures, the dominance of the peroxides is given away to the chain branching reaction (3.41). The same types of chemistry are relevant to higher alkanes.

(c) The dominant chemistry in each temperature region switches from each other gradually. In other words, the temperatures, quoted above, that divide the various chemistry regions are only approximate. Often these temperatures are highly dependent on reactor pressure and fuel-oxidizer composition;

(d) The oxidation of methane, carbon monoxide, and hydrogen share many of the same reactions. The most critical reactions have been

$$H\bullet + O_2 \rightarrow O\bullet + OH\bullet \,. \tag{3.41}$$

$$H\bullet + O_2 + M \rightarrow HO_2\bullet + M \,. \tag{3.45}$$

$$CO + OH\bullet \rightarrow CO_2 + H\bullet \,. \tag{3.62}$$

As we will show later, these reactions are equally critical to combustion processes of all hydrocarbon fuels, and as such the reaction mechanisms of hydrogen and carbon monoxide oxidation are subset of methane oxidation; the mechanism of methane oxidation is a subset of higher hydrocarbon oxidation. This understanding shows that the reaction mechanism of large, practical fuel combustion should be built in a hierarchical fashion;

(e) Most of the bimolecular reactions that appear in the reaction mechanisms just discussed involve a molecular species and a free radical species. Why aren't bimolecular reactions between two molecular species (e.g., $CH_4 + CH_2O \rightarrow$ products) or between two free-radical species (e.g., $HCO\bullet + CH_3\bullet \rightarrow$ products) equally important? The reason is that though molecular species tend to have large concentrations, the rate coefficient of their reactions tends to be small. This is because the activation energy of molecular reactions is often very larger. Conversely, the rate coefficient of a reaction between two free radical species is usually very large, owing to the reactivity of both radical species, but their concentrations are usually very small. Therefore, a compromise results in reactions between a molecule and a free radical being the fastest:

Reaction type	Concentrations		Rate Coefficient	Rate
	Reactant 1	Reactant 2		
Molecule + molecule	*large*	*large*	*very small*	***small***
Molecule + radical	*large*	*small*	*intermediate*	***large***
Radical + radical	*small*	*small*	*large*	***small***

Of course, if a free radical is relatively stable (e.g., $HO_2\bullet$ and $CH_3\bullet$), it can be present in a reactor in high concentrations and capable of reacting with itself. Examples include reactions (3.46) and (3.73).

(f) The mechanism of methane oxidation at high temperature is quite well understood and quantified. One of the popular models is the GRI-Mech, developed in the 90s for natural gas combustion. The readers may wish to visit http://www.me.berkeley.edu/gri_mech/ to examine the reaction mechanism and its performance.

3.2.7 The NTC Behavior of Higher Alkane Hydrocarbons

We now return to the peculiar NTC problem seen in Figure 3.8. The low temperature (300-400 °C) oxidation of propane starts with the chain initiation reaction,

$$C_3H_8 + O_2 \rightarrow i\text{-}C_3H_7\bullet\ (\mathrm{CH_3\text{-}CH\bullet\text{-}CH_3}) + HO_2\bullet\ , \tag{3.88}$$
$$C_3H_8 + O_2 \rightarrow n\text{-}C_3H_7\bullet\ (\mathrm{CH_2\bullet\text{-}CH_2\text{-}CH_3}) + HO_2\bullet\ . \tag{3.89}$$

The resulting propyl radicals ($C_3H_7\bullet$), denoted by $R\bullet$ hereafter, react with molecular oxygen with several possible outcomes:

$$R\bullet + O_2\ (+M) \rightarrow RO_2\bullet\ (+M), \tag{3.90}$$
$$R\bullet + O_2\ (+M) \rightarrow R'\bullet O_2H\ \ (+M), \tag{3.91}$$
$$R\bullet + O_2 \rightarrow \text{olefin} + HO_2\bullet. \tag{3.92}$$

Here the product olefin is an unsaturated hydrocarbon that has a double C=C bond, i.e., propene ($\mathrm{CH_3\text{-}CH{=}CH_2}$) in this case. There is conclusive evidence that the above reactions develop from a complex process that involve collision stabilization and isomerization of the $RO_2\bullet$ radical – a subject we shall discuss in somewhat more detail at a later time. For $n\text{-}C_3H_7\bullet$, this reaction process may be depicted by

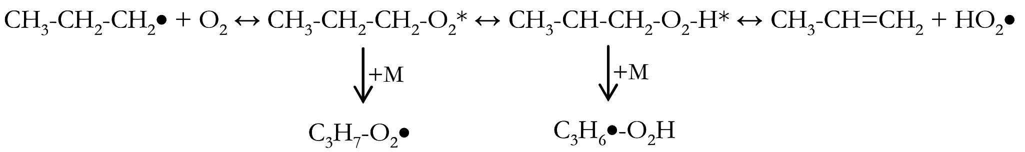

$$\begin{tikzcd}
\mathrm{CH_3\text{-}CH_2\text{-}CH_2\bullet + O_2} \arrow[r, leftrightarrow] & \mathrm{CH_3\text{-}CH_2\text{-}CH_2\text{-}O_2^*} \arrow[r, leftrightarrow] \arrow[d, "+M"] & \mathrm{CH_3\text{-}CH\text{-}CH_2\text{-}O_2\text{-}H^*} \arrow[r, leftrightarrow] \arrow[d, "+M"] & \mathrm{CH_3\text{-}CH{=}CH_2 + HO_2\bullet} \\
 & \mathrm{C_3H_7\text{-}O_2\bullet} & \mathrm{C_3H_6\bullet\text{-}O_2H} &
\end{tikzcd}$$

The $RO_2\bullet$ radical abstracts an H atom from RH to continue the chain reaction process,

$$RO_2\bullet + RH \rightarrow \mathrm{RO_2H} + R\bullet\ . \tag{3.93}$$

Chain branching is accomplished with the dissociation of $R\mathrm{O_2H}$, i.e.,

$$RO_2H\ (+M) \rightarrow RO\bullet + OH\bullet\ (+M). \tag{3.94}$$

Of course, the $OH\bullet$ radicals will attack the fuel to form more alkyl radicals,

$$RH + OH\bullet \rightarrow R\bullet + H_2O\ (+M). \tag{3.95}$$

The $RO_2\bullet$ radical can also undergo isomerization to form $R'\bullet\mathrm{OOH}$,

$$RO_2\bullet\ (+M) \rightarrow R'\bullet\mathrm{OOH}\ \ (+M), \tag{3.96}$$

which may react with molecular oxygen and in several steps, produces two reactive *OH*• radicals.*

What then causes the negative temperature coefficient behavior? The answer again lies in the stability of the *RO*$_2$• radical. Note that the reaction sequence, starting from the formation of *RO*$_2$• (3.90) to its subsequent reactions (3.93-96), is chain branching (path I), whereas the reaction (3.92) is only chain propagating (path II). Just like CH_3O_2•, as we increase the temperature, the *RO*$_2$• becomes less stable (owing to the reduction of entropy). It decomposes and reverts to *R*• and O_2. Consequently the chain branching path I becomes less competitive and the chain propagating path II becomes relatively more competitive. The net result is a decrease in the overall reactivity, or the NTC behavior seen in Figure 3.8.

The NTC behavior disappears by about 800 K. Above this temperature the H_2O_2 chemistry starts to play a role and the chain reaction sequence is replaced by the intermediate-temperature chemistry. The relevance of reactions (3.90-96) disappears, and so does the NTC behavior.

3.2.8 Engine Knock and Octane Number

The low and intermediate chemistry of alkane oxidation is important to the understanding of engine knock. As we know, SI engines operate with premixed and vaporized gasoline fuel and air. Assuming that prior to compression, the temperature and pressure of the engine are 400 K and 1 atm, respectively. After compression, the temperature and pressure reach about 900 K and 18 atm.* The data in Figure 3.8 clearly show that as we compress a straight-chain alkane fuel and air mixture, the mixture will spontaneously ignite before it can be fully compressed. This behavior is known as *engine knock*. It causes pre-mature ignition before the end of compression and spark ignition.

In early days, we used leaded gasoline, which contains a chemical known as tetraethyl-lead. The chemical is very effective to quench unwanted free radical species prior to spark ignition. It was realized in the late 60s and early 70s that tetraethyl-lead is poisonous. The unleaded gasoline that we use today contains a large amount of aromatics (ethylenebenzene etc) (~40% by weight), as aromatics are known to be resistant to low-temperature oxidation and alkyl aromatics can scavenge free radicals species formed prior to the completion of compression.

This brings the topic of the *Octane number* of a gasoline fuel. This number is usually measured from 0 to 100 scale. If an arbitrary fuel or fuel mixture has the engine knocking tendency of normal heptane (C_7H_{16}), its octane number is equal to 0 (maximum knocking). If the same fuel has the knocking tendency of 2,2,4-trimethylpentane (iso-octane, C_8H_{18}), its

---

[*] See Glassman, I. *Combustion*, 2nd Edition, Academic Press, San Diego, pp. 84-88.

[*] Recall that the compression ratio of a typical SI engine is 8 to 10. Adiabatic compression equations are $(P_2/P_1) = (V_1/V_2)^{\gamma}$ and $(T_2/T_1) = (V_1/V_2)^{\gamma-1}$, where $\gamma \approx 1.4$ for air.

octane number is assigned a value of 100 (minimal knocking). Octane numbers between 0 and 100 is determined by mixing normal pentane and iso-octane. That is, a fuel with an octane number of 88 has a knocking tendency equivalent to a mixture of 88% iso-octane and 12% normal heptane.

Table 3.1 shows the octane number of many single-component fuels. In general, the octane numbers may be ordered by

Straight alkanes < cycloalkanes < branched-chain alkanes ~ alkenes < aromatics .

The relative order between straight-chain alkanes and branched-chain alkanes is quite understandable. Alkyl radicals produced from branched-chain alkanes tend to be more stable than the primary and second radicals of straight chain alkanes. For example, we have

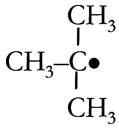

$$CH_3\text{–}\overset{CH_3}{\underset{CH_3}{C}}\bullet$$

Tert-butyl

$\bar{h}^{\circ}_{f,298}$ = 48 kJ/mol

$$CH_3\text{–}\overset{\bullet}{C}H\text{–}CH_2\text{–}CH_3$$

secondary butyl

$\bar{h}^{\circ}_{f,298}$ = 57 kJ/mol

$$\bullet CH_2\text{–}CH_2\text{–}CH_2\text{–}CH_3$$

primary butyl

$\bar{h}^{\circ}_{f,298}$ = 67 kJ/mol

Notice the order of the enthalpy of formation. The tert-butyl radical is quite stable by itself. For the same reason, the $RO_2\bullet$ radical, resulting from the addition of O_2 to radical, is quite unstable. It tends to reverse the course of reaction and dissociates to reactants $R\bullet$ and O_2. In this way, the oxidation of the parent *tert*-butane does not have the necessary chain branching step for ignition or explosion. On the other hand, the $RO_2\bullet$ radicals produced from the addition of O_2 to the primarily secondary butyl radicals are somewhat more stable, leading to rapid chain branching and hence compression ignition. There are additional kinetic effects resulting from the different free radical structures. These will not be discussed here.

Table 3.1 Octane number of pure fuels

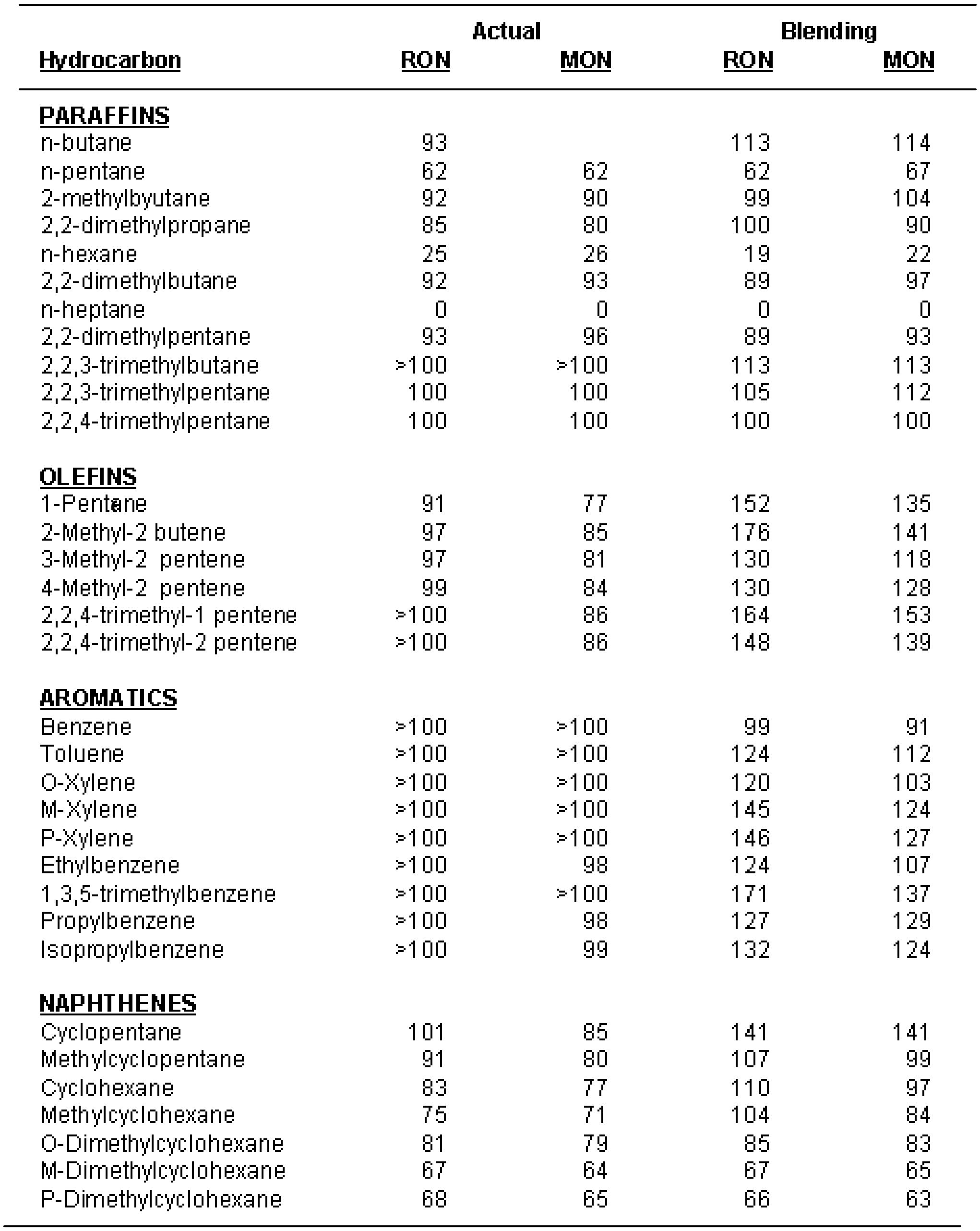

Hydrocarbon	Actual RON	Actual MON	Blending RON	Blending MON
PARAFFINS				
n-butane	93		113	114
n-pentane	62	62	62	67
2-methylbyutane	92	90	99	104
2,2-dimethylpropane	85	80	100	90
n-hexane	25	26	19	22
2,2-dimethylbutane	92	93	89	97
n-heptane	0	0	0	0
2,2-dimethylpentane	93	96	89	93
2,2,3-trimethylbutane	>100	>100	113	113
2,2,3-trimethylpentane	100	100	105	112
2,2,4-trimethylpentane	100	100	100	100
OLEFINS				
1-Pentane	91	77	152	135
2-Methyl-2 butene	97	85	176	141
3-Methyl-2 pentene	97	81	130	118
4-Methyl-2 pentene	99	84	130	128
2,2,4-trimethyl-1 pentene	>100	86	164	153
2,2,4-trimethyl-2 pentene	>100	86	148	139
AROMATICS				
Benzene	>100	>100	99	91
Toluene	>100	>100	124	112
O-Xylene	>100	>100	120	103
M-Xylene	>100	>100	145	124
P-Xylene	>100	>100	146	127
Ethylbenzene	>100	98	124	107
1,3,5-trimethylbenzene	>100	>100	171	137
Propylbenzene	>100	98	127	129
Isopropylbenzene	>100	99	132	124
NAPHTHENES				
Cyclopentane	101	85	141	141
Methylcyclopentane	91	80	107	99
Cyclohexane	83	77	110	97
Methylcyclohexane	75	71	104	84
O-Dimethylcyclohexane	81	79	85	83
M-Dimethylcyclohexane	67	64	67	65
P-Dimethylcyclohexane	68	65	66	63

Taken from http://www.refiningonline.com/EngelhardKB/crep/TCR4_29.htm. RON = Research Octane Number; MON = Motor Octane Number. RON simulates fuel performance under low severity engine operation. MON simulates more severe operation that might be incurred at high speed or high load. In practice the octane of a gasoline is reported as the average of RON and MON or R+M/2. Actual octane number refers to the performance of a pure fuel, whereas blending octane number refers the actual influence of a fuel to knocking for a specific gasoline composition.

3.2.8 Higher Alkane Oxidation at High Temperatures

The high-temperature oxidation of a straight chain hydrocarbon is quite easy to understand. When free radicals are abundant, their reactions with an alkane are exclusively the H-abstraction reactions, i.e.,

$$RH + (H\bullet,\ O\bullet\ \&\ OH\bullet) \rightarrow R\bullet + (H_2,\ OH\bullet,\ H_2O). \tag{3.97}$$

The alkyl radicals usually decompose thermally and rapidly. Take propane as an example. The initial H-abstraction reaction may lead to the formation of the *n*-propyl radical,

$$CH_3\text{–}CH_2\text{–}CH_3 + (H\bullet,\ O\bullet\ \&\ OH\bullet) \rightarrow CH_3\text{–}CH_2\text{–}CH_2\bullet + (H_2,\ OH\bullet,\ H_2O). \tag{3.98}$$

The resulting *n*-propyl radical will largely decompose following the β-scission rule, i.e.,

$$CH_3\text{–}CH_2\text{–}CH_2\bullet\ (+M) \rightarrow CH_3\bullet + C_2H_4\ (+M), \tag{3.99}$$

to yield the methyl radical and ethylene. In the case of *i*-propyl, the products of the above sequence of reactions would be propene and the $H\bullet$ atom,

$$CH_3\text{–}CH_2\text{–}CH_3 + (H\bullet,\ O\bullet\ \&\ OH\bullet) \rightarrow CH_3\text{–}CH\bullet\text{–}CH_3 + (H_2,\ OH\bullet,\ H_2O). \tag{3.100}$$

$$CH_3\text{–}CH\bullet\text{–}CH_3\ (+M) \rightarrow H\bullet + C_3H_6\ (+M), \tag{3.101}$$

The β-scission rule states that the weakest bonds in a free radical is the bond immediately removed from the bond connected to the free radical site. This rule is easily understood by considering the bond energies. Take the *n*-butyl radical as an example,

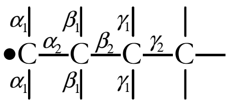

We label the bonds by α, β, γ etc, starting from the free radical site. Table 3.2 shows the dissociation products and bond energies in the *n*-butyl radical. Clearly the β_2 (C–C) bond is the weakest with bond energy equal to 104 kJ/mol. This is the bond that would be easily broken. The second weakest bond is the β_1 (C–H) bond (bond energy equal to 151 kJ/mol). The rest of the bonds are much stronger (>380 kJ/mol) and will remain intact even at very high temperatures. Therefore, in the case of the *n*-butyl radical, the preferred products of dissociation are largely ethylene and the ethyl radical,

$$CH_3\text{–}CH_2\text{–}CH_2\text{–}CH_2\bullet\ (+M) \rightarrow C_2H_5\bullet + C_2H_4\ (+M). \tag{3.102}$$

Since the ethyl radical does not have a β *C–C* bond, it prefers to break the β *C–H* bond , leading to the formation of ethylene and an $H\bullet$ atom.

Table 3.2 Dissociation products and bond energies in the *n*-butyl radical

Bond	Products	$D_{e,298\text{K}}$ (kJ/mol)
α_1	$CH_3\text{–}CH_2\text{–}CH_2\text{–}CH\text{:} + H$	~490
α_2	$CH_3\text{–}CH_2\text{–}CH_2\bullet + CH_2\text{:}$	~426
β_1	$CH_2{=}CH\text{–}CH_2\text{–}CH_3 + H\bullet$	151
β_2	$CH_2{=}CH_2 + CH_3\text{–}CH_2\bullet$	104
γ_1	$\bullet CH_2\text{–}CH_2\text{–}CH\bullet\text{–}CH_3 + H\bullet$	~413
γ_2	$\bullet CH_2\text{–}CH_2\text{–}CH_2\bullet + CH_3\bullet$	~383

$$C_2H_5\bullet\ (+M) \rightarrow C_2H_4 + H\bullet\ (+M). \qquad (3.103)$$

For the *i*-butyl radical, we have

$$CH_3\text{–}CH_2\text{–}CH\bullet\text{–}CH_3\ (+M) \rightarrow CH_3\bullet + C_3H_6\ (+M). \qquad (3.103)$$

Another example is the *n*-octyl radical.

$$\begin{aligned} &CH_3\text{–}CH_2\not-CH_2\text{–}CH_2\not-CH_2\text{–}CH_2\not-CH_2\text{–}CH_2\bullet\ (+M)\\ &\quad\rightarrow H\bullet + 4\ C_2H_4\ (+M). \qquad (3.104)\end{aligned}$$

The various *i*-octyl radicals do make things complicated though, e.g.,

$$\begin{aligned} &CH_3\not-CH_2\text{–}CH_2\not-CH_2\text{–}CH_2\not-CH_2\text{–}CH\bullet\text{–}CH_3\ (+M)\\ &\quad\rightarrow CH_3\bullet + 2\ C_2H_4 + C_3H_6\ (+M) \qquad (3.105)\end{aligned}$$

$$\begin{aligned} &CH_3\text{–}CH_2\not-CH_2\text{–}CH_2\not-CH_2\text{–}CH\bullet\text{–}CH_2\not-CH_3\ (+M)\\ &\quad\rightarrow H\bullet + 2\ C_2H_4 + C_4H_8\ (+M) \qquad (3.106a)\end{aligned}$$

or

$$\rightarrow CH_3\bullet + C_7H_{14}\ (+M). \qquad (3.106b)$$

Nonetheless, the resulting alkene molecules would undergo rapid dissociation, again following the *H*-abstration—***β***-scission sequence of reaction, e.g.,

$$CH_3\text{–}CH_2\text{–}CH{=}CH_2 + (H\bullet,\ O\bullet\ \&\ OH\bullet) \rightarrow \bullet CH_2\text{–}CH_2\text{–}CH{=}CH_2 + (H_2,\ OH\bullet,\ H_2O) \qquad (3.107)$$

$$CH_3\text{–}CH_2\text{–}CH{=}CH_2 + (H\bullet,\ O\bullet\ \&\ OH\bullet) \rightarrow CH_3\text{–}CH\bullet\text{–}CH{=}CH_2 + (H_2,\ OH\bullet,\ H_2O) \qquad (3.108)$$

$$\bullet CH_2\text{–}CH_2\text{–}CH{=}CH_2\ (+M) \rightarrow C_2H_3\bullet + C_2H_4\ (+M) \qquad (3.109)$$

$$CH_3\text{–}CH\bullet\text{–}CH{=}CH_2\ (+M) \rightarrow H\bullet + C_4H_6\ (+M) \qquad (3.110)$$

where C_4H_6 is the butadiene molecule ($CH_2{=}CH\text{–}CH{=}CH_2$).

With the above discussion it becomes clear that upon the initial *H*-abstraction (3.97), a straight chain alkane molecule would mostly decompose to small fragments following the ***β***-

scission rule. These fragments include mainly the $H\bullet$, $CH_3\bullet$, and small alkene molecules, C_2H_4, C_3H_6, and C_4H_6.

3.2.9 The Oxidation of Ethylene and Other Alkene Compounds

Although very few alkene compounds are present in real fuels, the oxidation of alkene is important to combustion chemistry. In general, alkenes are major intermediates of combustion. They are often formed as the result of β-scission reactions of larger alkyl radicals. In addition, under the fuel rich condition, the oxidation of methane also leads to ethylene formation through the recombination of the methyl radicals,

$$CH_3\bullet + CH_3\bullet\ (+M) \rightarrow C_2H_6\ (+M) \qquad (3.111)$$

$$CH_3\bullet + CH_3\bullet \rightarrow C_2H_5\bullet + H\bullet \qquad (3.112)$$

$$C_2H_6 + (H\bullet,\ O\bullet\ \&\ OH\bullet) \rightarrow C_2H_5\bullet + (H_2,\ OH\bullet,\ H_2O) \qquad (3.113)$$

$$C_2H_5\bullet\ (+M) \rightarrow C_2H_4 + H\bullet\ (+M). \qquad (3.114)$$

Unlike the single σ C–C and C–H bond in alkanes, the π bond in ethylene is susceptible to attack by the $O\bullet$ atom,

$$C_2H_4 + O\bullet \rightarrow CH_3\bullet + HCO\bullet. \qquad (3.115)$$

In addition, the H-abstraction of C_2H_4 by the $H\bullet$ and $OH\bullet$ radical leads to the formation of the vinyl ($C_2H_3\bullet$) radical,

$$C_2H_4 + (H\bullet\ \&\ OH\bullet) \rightarrow C_2H_3\bullet + (H_2\ \&\ H_2O), \qquad (3.116)$$

which is oxidized through

$$C_2H_3\bullet + O_2 \rightarrow CH_2O + HCO\bullet \qquad (3.117)$$

$$C_2H_3\bullet + O_2 \rightarrow CH_2CHO\bullet + O\bullet \qquad (3.118)$$

$$CH_2CHO\bullet\ (+M) \rightarrow CH_3O\bullet + CO\ (+M). \qquad (3.119)$$

We see that the products of the above reactions are basically the intermediates of methane oxidation. The rest of the reaction mechanism is therefore identical to that of methane (see, section 3.2.6).

Under the fuel rich conditions, the lack of sufficient molecular oxygen means that reactions (3.117) and (3.118) would be quite slow. Therefore the vinyl radical undergoes thermal decomposition to yield acetylene,

$$C_2H_3\bullet\ (+M) \rightarrow C_2H_2 + H\bullet\ (+M). \qquad (3.120)$$

Thermodynamically acetylene is always favored as an end product, in addition to CO and solid carbon, under the fuel rich combustion of hydrocarbon fuels.

In the case of propene (C_3H_6), the combustion reactions are

$$C_3H_6 + H\bullet \rightarrow C_2H_4 + CH_3\bullet \tag{3.121}$$
$$C_3H_6 + O\bullet \rightarrow CH_2CHO\bullet + CH_3\bullet \tag{3.122}$$
$$C_3H_6 + O\bullet \rightarrow C_2H_5\bullet + HCO\bullet. \tag{3.123}$$

For butadiene (C_4H_6), we have

$$C_4H_6 + H\bullet \rightarrow C_2H_4 + C_2H_3\bullet \tag{3.124}$$

3.2.10 The Chemistry of Acetylene

As we discussed earlier, acetylene is a fairly energetic fuel. Acetylene is also one of the major intermediates of fuel-rich combustion. The source of acetylene is primarily reaction (3.120). If a pocket of fuel rich mixture is mixed with air, the oxidation of acetylene proceeds mostly through

$$C_2H_2 + O\bullet \rightarrow HCCO\bullet + H\bullet \tag{3.125}$$
$$C_2H_2 + O\bullet \rightarrow CH_2\bullet + CO \tag{3.126}$$
$$HCCO\bullet + H\bullet \rightarrow CH_2\bullet(\mathrm{S}) + CO \tag{3.127}$$
$$HCCO\bullet + O\bullet \rightarrow H\bullet(\mathrm{S}) + 2CO \tag{3.128}$$
$$CH_2\bullet(\mathrm{S}) + M \rightarrow CH_2\bullet + M \tag{3.129}$$
$$CH_2\bullet + O_2 \rightarrow HCO\bullet + OH\bullet\,. \tag{3.84}$$

Here $CH_2\bullet$(S) is the electronically excited $CH_2\bullet$ radical.

The chemistry of acetylene has attracted significant attentions over the last few decades. The principal reason is that in the presence of the $H\bullet$ and $O\bullet$ atoms, it can polymerize to aromatics in flames, which subsequently produces soot (or smoke).

3.3 Pollutants Formation

A principal reason why combustion chemistry is important to us is because of pollutant formation. Today, one cannot design a combustion engine without considering pollutant emission.

The major pollutants emitted from fossil-fuel combustion include hydrocarbons (HC), carbon monoxide (CO), nitrogen oxides (NO_x), sulfur oxides (SO_x), particulates (soot/smoke), and carbon dioxide (CO_2). Table 3.3 summarizes the sources and effects of these air pollutants.

Table 3.3 Primary Sources of Air Pollutants

Pollutant	Combustion sources	Other sources	Major effects
HC	Gasoline engines Incineration Fires	Fuel evaporation Organic solvents	Photochemical smog Reduced combustion efficiency Green house effects
CO	Gasoline engines	Industrial process	Toxic, lethal at high dosages photochemical smog
NO_x	Motor vehicles	Chemical processes	Photochemical smog Acid rain Respiratory illness Skin and eye irritation
SO_x	Electricity generation Industrial boilers	Chemical processes	Acid rain Respiratory illness
Particulates (soot)	Electricity generation Diesel engines		Global climate Toxic (skin cancer) Respiratory illness
CO_2	All hydrocarbon combustion	Deforestation	Green house effects

3.3.1 Type and Effects of Air Pollution

A good source of information about types of air pollutants and their effects may be found on the web site of the U.S. Environmental Protection Agency (EPA):

http://www.epa.gov/air/topics/comeap.html

3.3.1.1 Acid rain

Acid rain is formed from mixing SO_x and NO_x with rain droplets. In general the condensation of water vapor initially leads to clouds/rain droplets that are neutral in acidity. Our "*natural*" atmosphere is rich in CO_2 (~280 PPM prior to industrial revolution and ~380 PPM today). CO_2 is partially soluble in water, forming carbonic acid (H_2CO_3). Therefore, natural rain water is acidic with a Ph level equal to 5.6 (Neutral water has Ph = 7). Acid rain is defined as rain water with Ph < 5.6. The following chart demonstrates the Ph level of various liquids:

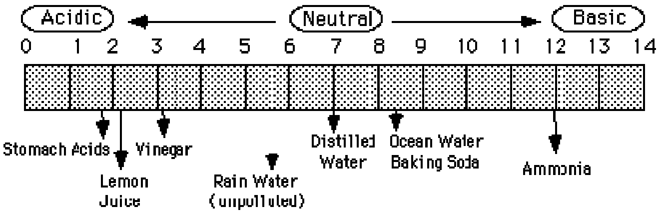

In general, acid rain problem is more severe in the eastern part of the U.S where the Ph level of rain water is around ~ 4.5. In some regions, a Ph level of 3 is common. The principal cause is coal combustion.

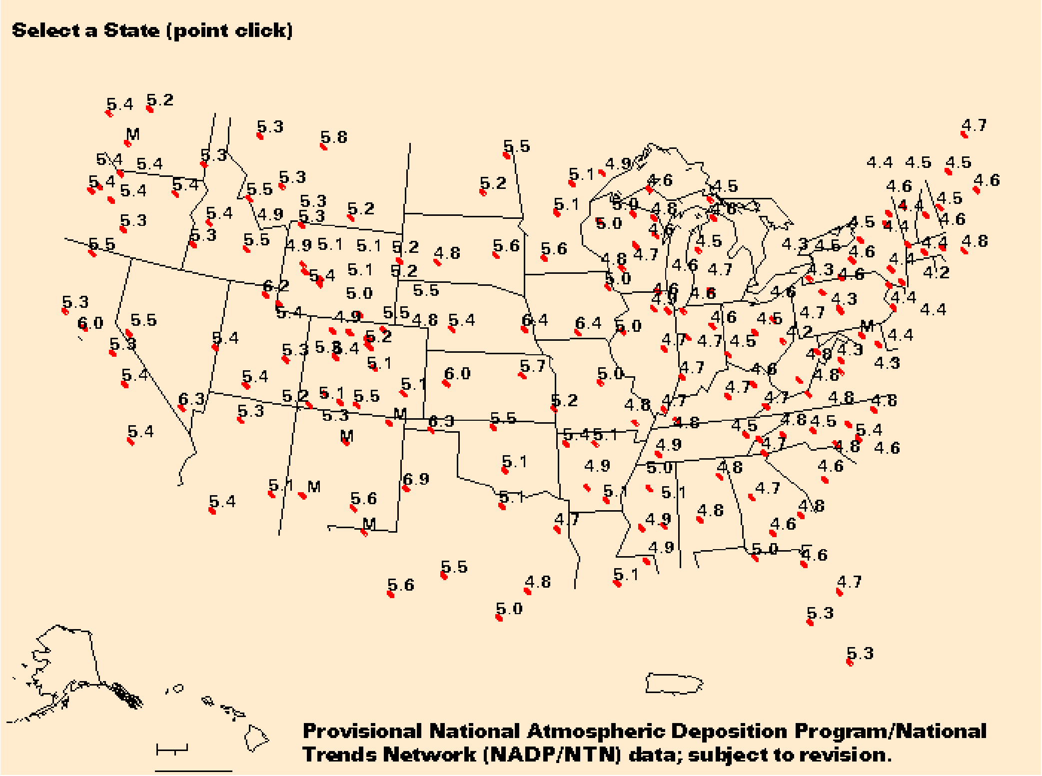

Figure 3.10. pH of Precipitation for November 26, - December 23, 2001 (taken from http://water.usgs.gov/nwc/NWC/pH/html/ph.html)

Acid rain causes acidification of lakes and streams and contributes to damage of trees at high elevations (for example, red spruce trees above 2,000 feet) and many sensitive forest soils. In addition, acid rain accelerates the decay of building materials and paints, including irreplaceable buildings, statues, and sculptures that are part of our nation's cultural heritage. Prior to falling to the earth, SO_2 and NO_x gases and their particulate matter derivatives, sulfates and nitrates, contribute to visibility degradation and harm public health.

http://www.epa.gov/air/topics/comeap.html

3.3.1.2 Photochemical Smog

Photochemical smog is caused by complex atmospheric reactions of NO_x, hydrocarbons and oxygen under the irradiation of sunlight. In ambient air, the principal mechanism of photochemical smog formation is thought to be the following sequence of chain reactions:

$$NO_2 + h\nu \rightarrow NO + O\bullet \tag{3.130}$$
$$O_2 + O\bullet + M \rightarrow O_3 + M \tag{3.131}$$
$$NO + O_3 \rightarrow NO_2 + O_2 \tag{3.132}$$

where $h\nu$ denotes a photon. The important feature of the above chain reaction is that it generates a background ozone and the $O\bullet$ atom in the ambient air. But since ozone is produced and destroyed at almost the equal rates through reactions (3.131) and (3.132), there is no net accumulation of O_3, unless NO is oxidized to NO_2 by other species. To this end, the presence of volatile organic compounds (VOCs) and carbon monoxide is an element critical to photochemical smog. Specifically, the $O\bullet$ atom can react with water vapor to form the hydroxyl radical,

$$O\bullet + H_2O \rightarrow OH\bullet + OH\bullet \tag{3.61}$$

In ambient air, carbon monoxide reacts with the hydroxyl radical in the same way as that in combustion, i.e.,

$$CO + OH\bullet \rightarrow CO_2 + H\bullet \tag{3.62}$$

and the resulting $H\bullet$ atom combines with O_2 for form the hydrogen peroxy radical,

$$H\bullet + O_2 + M \rightarrow HO_2\bullet + M \tag{3.45}$$

Consequently another route to NO oxidation becomes relevant,

$$NO + HO_2\bullet \rightarrow NO_2 + OH\bullet \tag{3.133}$$

Clearly, the aforementioned reaction steps form a chain reaction cycle with the net result of ozone production. It is ozone that causes a variety of health problems stated in Table 3.3.

The mechanism of NO oxidation catalyzed by VOCs is not completely understood. It is known, however, that VOCs again catalyze the oxidation of NO though the hydrocarbon peroxy radical. In the case of methane, the following reactions take place in the ambient air

$$CH_4 + OH\bullet \rightarrow CH_3\bullet + H_2O \tag{3.63}$$
$$CH_3\bullet + O_2\ (+M) \rightarrow CH_3O_2\bullet\ (+M) \tag{3.64}$$
$$CH_3O_2\bullet + NO \rightarrow CH_3O\bullet + NO_2 \tag{3.134}$$
$$CH_3O\bullet + O_2 \rightarrow CH_2O + HO_2\bullet \tag{3.74}$$
$$CH_2O + h\nu \rightarrow HCO\bullet + H\bullet \tag{3.135}$$
$$HCO\bullet + O_2 \rightarrow CO + HO_2\bullet \tag{3.76}$$

Clearly, the above sequence of reactions (a) converts NO to NO_2 through (3.134) and (b) yields additional $HO_2\bullet$ radicals that speed up the oxidation of NO.

3.3.1.3 Particulate Matters

Combustion generated *particulate matters* (PM) are usually fine particles with sizes $< \sim 1\ \mu$m. Soot or smoke represents a significant source of particular air pollutants. In general, particulates can be suspended in the air for long periods of time. Analyses show that increased hospitalizations for cardiovascular and lung diseases are linked to high levels of particle pollution.

In addition to human health hazards, PM have also been linked to changes in local air quality and global climate. For example, soot has a good light absorber and can increase the absorption of sunlight by ambient air. On the other hand, soot is may also serve as cloud condensation nuclei, which increase the global cloud density. The formation of contrail is believed, to an extent, to be induced by water condensation on oxidized soot particles.

3.3.1.4 Green House Gases

Combustion generated green-house gases include mainly carbon dioxide and methane. Other major greenhouse gases include water vapor, nitrous oxide (N_2O), ozone, and chlorofluoro carbons (CFCs). These gases have been related to the potential of global warming.

The *greenhouse effect*, first proposed by Joseph Fourier in 1824, is the process by which an atmosphere warms a planet. Figure 3.11 illustrates this effect. Since the sun is roughly a black body, its radiation is the most intense in the yellow wavelength region. Solar radiation that passes though the atmosphere is either absorbed by the earth surface or scattered back into the space. The earth is cooled by radiating back into the space in the infrared range. Gases like H_2O and CO_2 are transparent to visible radiation but are not transparent with respect to infrared radiation. In other words, the absorption of infrared and re-radiation by CO_2 leads to a net absorption of energy on the earth surface and in the lower atmosphere.

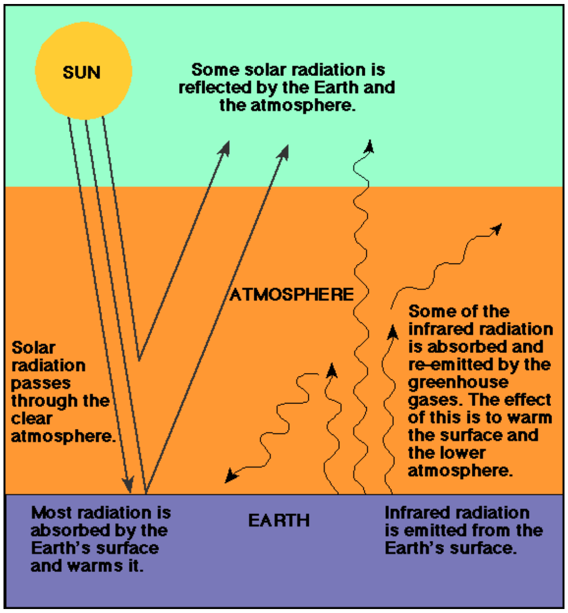

Figure 3.11. Schematic illustration of the green house effect in global warming (adapted from http://www.crystalinks.com/greenhouseeffect.html).

The average surface temperature would be –18°C without water, carbon dioxide, or other grean house gases. In reality this temperature is closer to 15°C due to the presence of natural green house gases (as well as convective flow of heat energy within the atmosphere). Obviously, an increase in CO_2 concentration due to human activities can enhance the "green house" effect and causes global warming.

Historically there is a clear correlation between the atmospheric CO_2 level and earth's surface temperature. Figure 3.12 shows the atmospheric CO_2 concentration (middle) and temperature (top) changes from the present (1950) over the past 400,000 years. There are several observations one can immediately make by examining these plots. First, the correlation between atmospheric CO_2 concentration and temperature is evident. Second, the variation of temperature over the last 400,000 years is well within ±5 °C. During this period of time, there are several occurrence of "ice age" when significant glacier advances were observed.

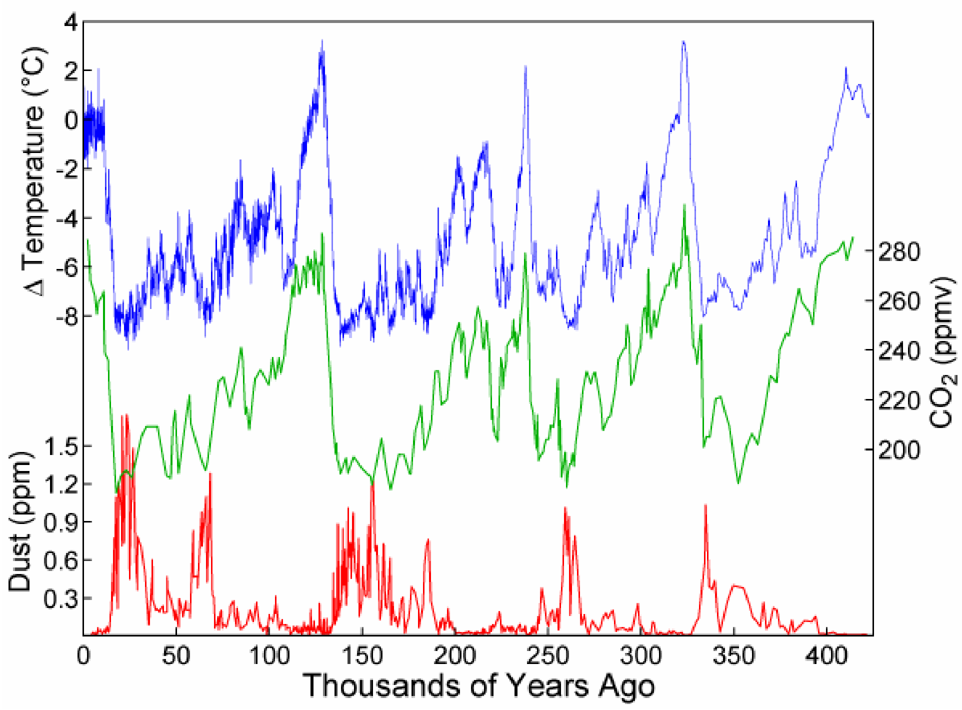

Figure 3.12 Variation of temperature (top), CO_2 (middle), and dust (bottom) levels over the last 400,000 years (adapted from http://en.wikipedia.org/wiki/Image:Ice_Age_Temperature.png).

There is clear evidence that atmospheric CO_2 concentration is rising rapidly since the time of industrial revolution. Figure 3.13 shows the variation of atmospheric CO_2 concentration over the last 250 years. Prior to industrial revolution, the CO2 concentration was roughly 280 PPM. Today, the level stands at 375 PPM, or a 34% increase over a relatively short period of time. Nearly all of the increase in CO_2 concentration is attributable to anthropogenic emission. In addition, Figure 3.14 shows that the concentrations of other green houses also rise quite rapidly over the last 150 years. Meanwhile, there is an exponential increase of temperature, starting right around 1900 (see, Figure 3.15).

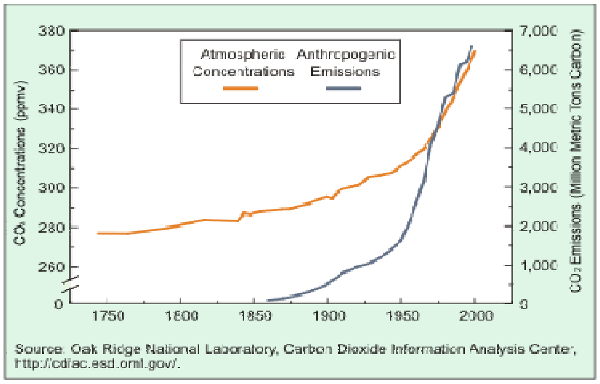

Source: Oak Ridge National Laboratory, Carbon Dioxide Information Analysis Center, http://cdiac.esd.ornl.gov/.

Figure 3.13 Variation of CO_2 concentration over the last 250 years.

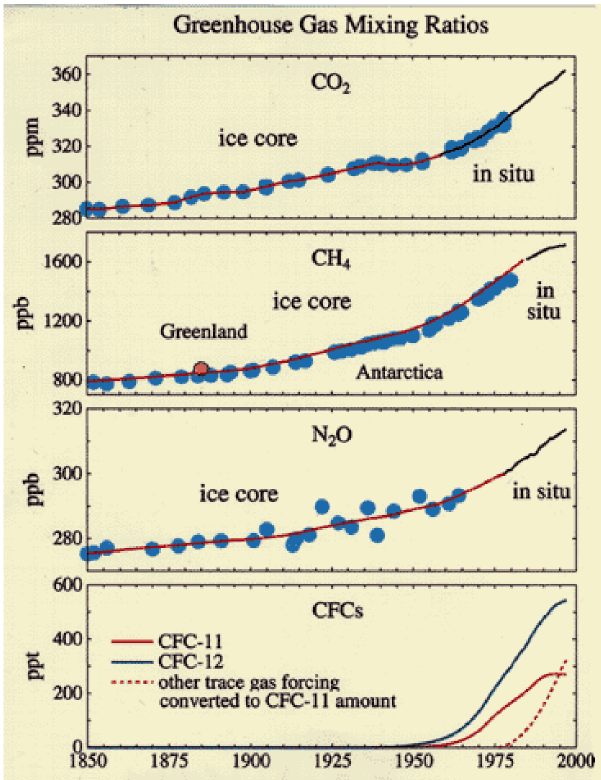

Figure 3.14 Concentrations of CO_2, CH_4, N_2O and CFCs over the last 150 years (adapted from http://www.agu.org/eos_elec/99148e.html).

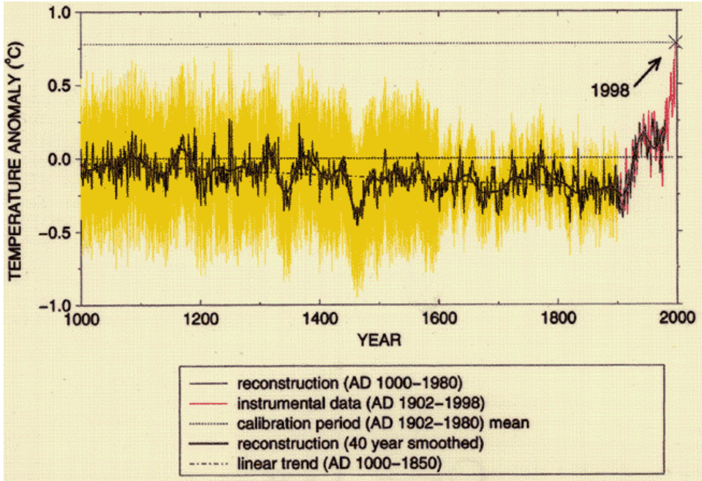

Figure 3.15 Temperature anomaly occurred from 1900 to 2000 (adapted from http://www.agu.org/eos_elec/99148e.html).

3.3.2 Mechanisms of Pollutant Formation in Fossil Fuel Combustion

We shall focus our discussion here to NO_x and soot formation. SO_x is normally formed from the oxidation of sulfur-containing compounds in fossil fuels. Reducing SO_x emission involves mostly fuel cleaning and flue gas scrubbing. These will not be discussed here.

3.3.2.1 Nitrogen oxides formation

Sources of NO_x from combustion may be categorized by fuel NO_x, thermal NO_x and prompt NO_x. Fuel NO_x is formed because of fossil fuels normally contains a certain amount of nitrogen. Upon combustion, fuel nitrogen is quickly released and oxidized into NO. The formation of thermal and prompt NO_x is related to the high-temperature reaction mechanism of hydrocarbons. In all three mechanisms, NO is directly produced in combustors, whereas NO_2 is formed as the result of NO oxidation in lower-temperature flue gases and in ambient air.

The concept of thermal NO_x was advanced by Zeldovich, who postulated that at high temperatures a chain reaction mechanism may be established as follows:

$$O_2 + M \rightarrow 2O\bullet + M \tag{3.136}$$

$$N_2 + O\bullet \rightarrow NO + N\bullet \tag{3.137}$$

$$N\bullet + O_2 \rightarrow NO + O\bullet \tag{3.138}$$

Of course, in combustion the $O\bullet$ atom is readily available (through the chain reaction $H\bullet + O_2 \rightarrow OH\bullet + O\bullet$). Consequently the formation of NO is intrinsic to hydrocarbon combustion. In addition, the hydroxyl radical is known to react with the $N\bullet$ atom, again yielding NO,

$$N\bullet + OH\bullet \rightarrow NO + H\bullet \tag{3.139}$$

In general, high temperature combustion operation favors the formation of thermal NO.

Prompt (Fenimore) NO is due to reactions of combustion intermediates $CH\bullet$ and $CH_2\bullet$ with molecular nitrogen. The following reaction sequence is believed to be responsible for additional NO production:

$$CH_2\bullet + N_2 \rightarrow HCN + NH\bullet \tag{3.140}$$

$$CH\bullet + N_2 \rightarrow HCN + N\bullet \tag{3.141}$$

$$NH\bullet + H\bullet \rightarrow N\bullet + H_2 \tag{3.142}$$

$$HCN + O\bullet \rightarrow NCO\bullet + H\bullet \tag{3.143}$$

$$NCO\bullet + H\bullet \rightarrow NH\bullet + CO \tag{3.144}$$

$$N\bullet + OH\bullet \rightarrow NO + H\bullet \tag*{(3.139)}$$

$$N\bullet + O_2 \rightarrow NO + O\bullet \tag*{(3.138)}$$

3.3.2.2 Soot formation

Soot forms as the result of local or global fuel-rich combustion. In liquid or solid hydrocarbon combustion, there always exist local environments that are fuel rich. Therefore soot formation is intrinsic to liquid and solid combustion.

Physically, soot is a graphite-like material with atomic C-to-H ratio ranging from 8 to 12. The mass density of soot is typically 1.8 g/cm^3, smaller than that of graphite (2.25 g/cm^3). Under high-resolution electron microscopy, soot appears to be fractal-like aggregates with dimension typically around 1 μm. These aggregates usually consist of hundreds of smaller, nearly spherical *primary* particles (Figure 3.16). The primary particles usually range in diameter from 20 to 50 nm. The bulk of soot mass is in the form of polycyclic aromatic hydrocarbons (PAHs). Depending on the process with which soot is formed, these PAHs can contain from 4 condensed aromatic rings to very large aromatic units, as in carbon black. Since PAH molecules are planar, they can stack on top of each other much like graphite, in which "infinitely large" PAHs are arranged in a layered fashion, with the interlayer distance equal to 3.347 Å. In contrast, the PAH interlayer spacing is between 3.4 and 3.6 Å.

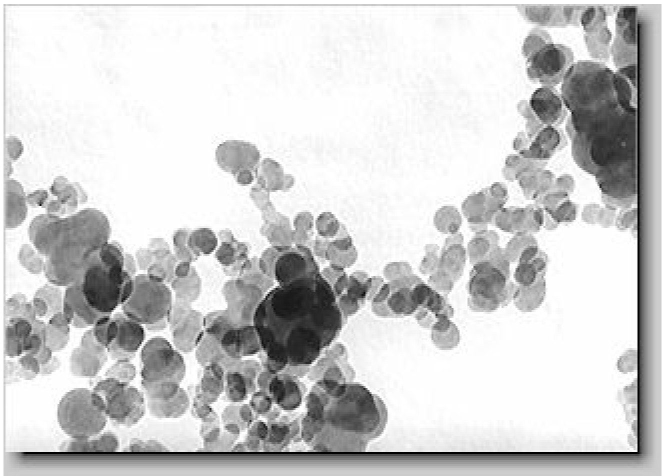

Figure 3.16 Typical soot aggregates (magnification = 100,000) (Adapted from http://www.a-m.de/englisch/lexikon/russ-bild1.htm).

Thermodynamically, soot formation is the consequence of entropy release. Upon heating, all hydrocarbons have the tendency to form coke (black carbon). Take propane as an example, the global reaction

$$C_3H_8 \rightarrow 3\ C(\text{solid}) + 4\ H_2 \tag{3.145}$$

is endorthermic by 104 and 127 kJ/mol at 300 and 2000 K, respectively, assuming that the solid carbon is graphite. However, the production of 4 moles of H$_2$ per mole of propane greatly increases the entropy, e.g., $T\Delta s^\circ_{300K} = 81$ kJ/mol and $T\Delta s^\circ_{2000K} = 641$ kJ/mol. The resulting Gibbs function of reaction is $\Delta G_r^\circ(300\text{ K}) = 23\,\text{kJ}$ per mole of propane, and $\Delta G_r^\circ(2000\text{ K}) = -514\,\text{kJ}$. Here we see that at the room temperature, the formation of solid carbon is not favored because the Gibbs function of reaction increases. At 2000 K, however, the Gibbs function of reaction is highly negative, indicating that the reaction is spontaneous. The driving force is, of course, the rise in entropy due to hydrogen release. In fact, carbon or soot is merely the byproduct of entropy maximization.

Kinetically the amount of soot formed often exceeds the thermodynamic prediction. This means that soot formation is a chemical kinetic problem and it requires a consideration of the underlying reaction mechanism. Figure 3.17 shows a bottom-up reconstruction of various complex processes that lead to soot formation. It shows that in the early stage of soot formation, PAHs are formed from unburned hydrocarbon intermediates (i.e., the ring compounds in the figure). These "2-dimensional" PAHs coalescence, physically or chemically, into "3-dimensional" clusters of PAH. This process is known as *particle nucleation* or *particle inception*. The clusters undergo further coagulation and coalescence to form spherical particles of a few nanometers in diameter. *Mass growth* of particles is accomplished largely through the reactions of gas-phase hydrocarbon species (e.g., acetylene) with soot surfaces, until particles assume a size of 20-50 nm, beyond which particles aggregate into fractal like structures, as seen in Figure 3.17.

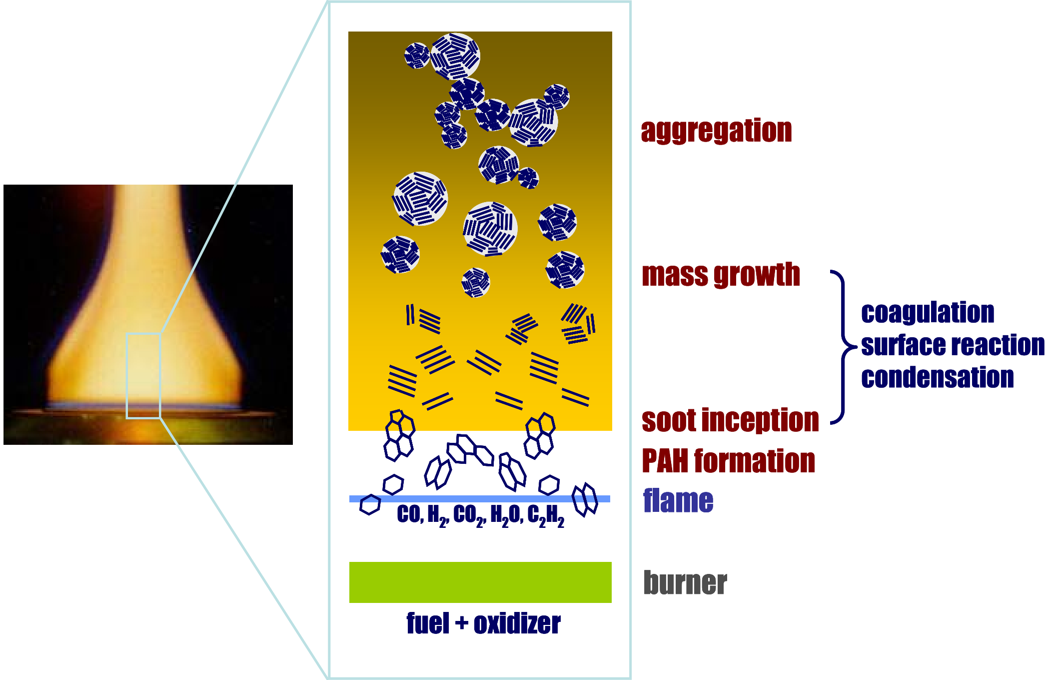

Figure 3.17 Elementary processes of soot formation.

In section 3.2.10, we discussed that acetylene is one of the major combustion intermediates under the fuel rich condition. Acetylene is known to undergo polymerization at high temperature. In combustion environments, the *H•* atom catalyzes this polymerization process. In the simplest form, the formation and growth of aromatics is described by the hydrogen-abstraction—carbon addition (HACA) mechanism. Since acetylene is usually the most abundant hydrocarbon species, the carbon addition is accomplished through acetylene. Figure 3.18 depicts a sequence of HACA reactions that lead to the formation and growth of aromatics in combustion. The mechanism features the polymerization of acetylene, mediated by the *H•* atom. The repetitive sequence of reactions involves the activation of a molecular species through the H-abstraction reaction, which produces a more reactive free radical species. Acetylene then adds to this free radical species, i.e.,

$$R\text{-}H + H\bullet \rightarrow R\bullet + H_2 \tag{3.146}$$

$$R\bullet + H\bullet \rightarrow R\text{-}H \tag{3.147}$$

$$R\bullet + C_2H_2 \rightarrow R'\text{-}H + H\bullet \text{ or } R'\bullet\,. \tag{3.148}$$

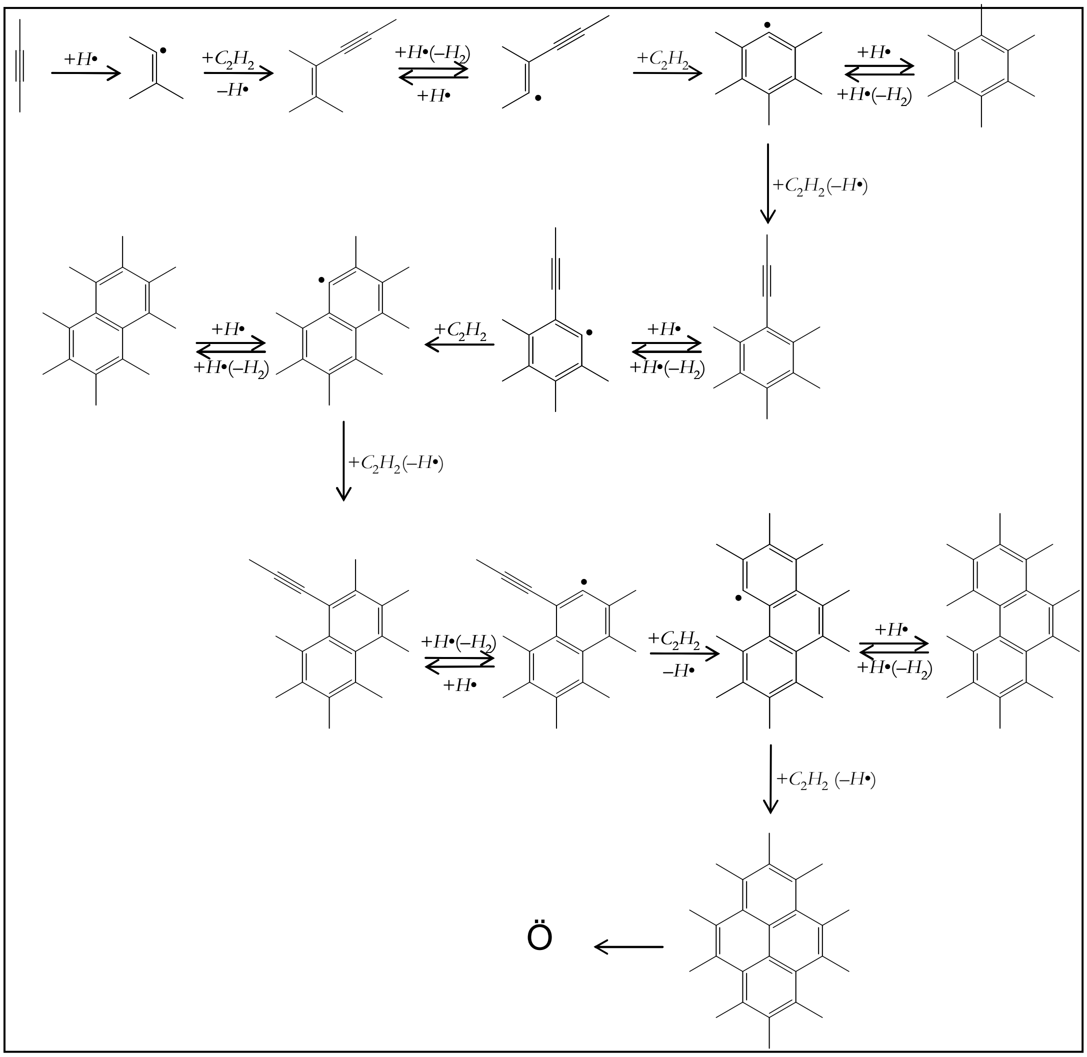

Figure 3.18 The Hydrogen-Abstraction—Carbon(acetylene)-Addition (HACA) mechanism of aromatics formation and growth.

In addition to the HACA mechanism, the first aromatic ring may form from the recombination of the propargyl radical ($H_2C{=}C{=}C\bullet H$, $C_3H_3\bullet$), i.e.,

$C_3H_3\bullet + C_3H_3\bullet \rightarrow$ 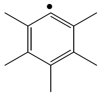 $+ H\bullet$. (3.149a)

$C_3H_3\bullet + C_3H_3\bullet \rightarrow$ 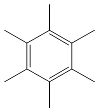 . (3.149b)

Propargyl belongs to a class of *resonantly stabilized* free radicals that are relatively stable than *non-resonantly stabilized* free radicals (see the explanation in the box below). For this reason, the propargyl radicals can have fairly high concentration in flames (reaching a level of 10^3 to 10^4 PPM). The source of the propargyl radical is the reaction of methylene ($CH_2\bullet$) radicals with acetylene, i.e.,

$$CH_2\bullet + C_2H_2 \rightarrow C_3H_3\bullet + H\bullet \qquad (3.150)$$

where under the fuel-rich condition the methylene radical is produced from

$$C_2H_2 + O\bullet \rightarrow CH_2\bullet + \mathrm{CO}\ . \qquad (3.151)$$

In resonantly stabilized radical species the electron resonance arises from the fact that the electron density of the free radical site is larger than that of a single, unpaired electron. A simple rule to identify resonance stabilization is to find all molecular structures of a given free radical species that do not violate the bonding rules. For example, the propargyl radical may be drawn in two forms, both of which are valid:

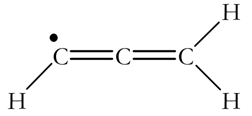

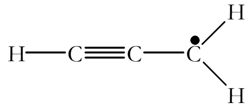

Thus the free radical site can be on both end carbon atoms. This behavior causes dynamic resonance in the electronic structure and in doing so it reduces both free radical site to molecule-like. Other examples include one of the $C_4H_3\bullet$ radicals ($HC{\equiv}C{-}C\bullet{=}CH_2$, i-C_4H_3)

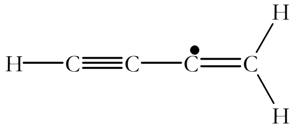

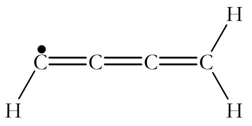 .

On the other hand, the other $C_4H_3\bullet$ radical isomer ($HC{\equiv}C{-}CH{=}CH\bullet$, n-C_4H_3) does not have resonance stabilization since there is only on way to draw its molecular structure, i.e.,

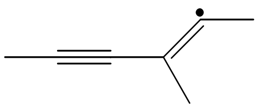

The benzene molecule grows in size in more or less the same way as how it is made itself. The aromatic structures presented in Figure 3.18 represent the most thermodynamically stable form of multiple-ring aromatics. The sequential reaction steps eventually lead to the formation of large aromatics or PAHs.

When PAH molecules become large enough, they start to coalesce into each other, forming PAH clusters (i.e., stacks of PAHs). The exact mechanism of the coalescence process is still unclear. Nonetheless experimental studies show that the process is rather rapid, to an extent that a direct measurement for particle inception is almost impossible. The clusters then grow by coagulating into each other, leading to particles that are a few nanometers in diameter. These processes may be physically depicted by the following sequence of reaction-like steps:

$$A_1 + A_1 \rightarrow B_2 \tag{3.152a}$$
$$A_1 + B_2 \rightarrow B_3 \tag{3.152b}$$
……
$$A_1 + B_n \rightarrow B_{n+1} \tag{3.152c}$$
……
$$B_2 + B_2 \rightarrow B_4 \tag{3.152d}$$
……

Here A_1 denotes a PAH molecule, B_2 is a dimer of PAH molecules, B_3 is a trimer and so on. Overall these processes require the sticking of PAHs and clusters upon their collision.

The majority of soot mass, however, is acquired through gas-surface reactions. Since the surface of soot particles is aromatic in nature, the HACA mechanism depicted in Figure 3.18 is equally applicable to the reactions between soot, the $H\bullet$ atom and acetylene. This surface reaction mechanism is often written as

$$S_i\text{-}H + H\bullet \rightarrow S_i\bullet + H_2 \tag{3.153}$$
$$S_i\bullet + H\bullet \rightarrow S_i\text{-}H \tag{3.154}$$
$$S_i\bullet + C_2H_2 \rightarrow S_{i+2}\text{-}H + H\bullet \tag{3.155}$$

With the mechanistic description given above, it is now possible to simulate the soot mass with detailed chemistry models. Yet owing to the complexity of the reaction mechanism of PAH formation, particle nucleation and growth, there are many scientific questions that remain unresolved. Usually the uncertainty in these soot models leads to an error of several factors in the predicted soot mass. These models have nonetheless gone into engine designers over the last decade with some success.